Drought and methyl jasmonate memory interact to determine plant functioning under current drought stress in a perennial grass

Tarun Bhatt[1*], Nikita Rathore[2], Jaroslav Semerad[3], Tomas Cajthaml[3], Dinesh Thakur[2], Zuzana Münzbergová[1,2]

[1]Department of Botany, Faculty of Sciences, Charles University, Benatska 2, 12800, Prague, Czech Republic, 12800

[2]Institute of Botany, Czech Academy of Sciences, Zamek 1,25243, Pruhonice, Czech Republic

[3]Institute of Microbiology of the Czech Academy of Sciences, Videnska 1083, 142 20 Prague, Czech Republic

*Corresponding author e-mail: bhatttarun954@gmail.com

Abstract

Climate-driven droughts necessitate deeper insights into plant resilience, particularly in clonal perennials. This study presents the first integrative analysis of how recurrent drought (D2), drought memory (D1), and methyl jasmonate-induced memory (M1) independently and interactively shape metabolomic diversity, composition, and morpho-physiological traits. Using *Festuca rubra* as a model species and using a full-factorial design, we found that current drought (D2) was the primary driver of metabolic reprogramming, reducing metabolite richness but enhancing uniqueness, suggesting a streamlined, stress-optimized strategy. D1 and M1 had significant, context-dependent impacts: D1 increased richness under well-watered conditions but reversed under drought, while M1 stabilized both metabolomic and trait variability. Importantly, D1 and M1 effects were non-additive, producing emergent biochemical states and morpho-physiology. A significant D1 × D2 × M1 interaction revealed complex integration of environmental and hormonal legacies. The metabolomic shifts closely aligned with traits such as specific leaf area and relative water content, indicating a coordinated adaptation at both metabolomic and morpho-physiological levels through memory-driven

mechanisms. Our findings confirm that both drought and hormone induced memories are transgenerational and compositional, with synergistic roles in plant stress adaptation. This suggests that combining hormonal and environmental priming strategies may be a viable approach to enhancing plant resilience under increasing climate variability.

Keywords: Metabolomics, methyl jasmonate, MeJA memory, drought resilience, clonal plants, transgenerational effects, phenotypic plasticity, drought memory, *Festuca rubra*.

1 Introduction

Plants are experiencing rapidly changing environments and face various stress factors, which can impact their growth and reproduction (Crisp et al., 2016). Drought stress is among the most significant stresses affecting plant growth and productivity worldwide (Michaletti et al., 2018). The 2023 IPCC report indicates that under projected climate change, drought events will occur more frequently and become more severe, threatening the structure, function, and productivity of ecosystems. Therefore, understanding the effects of drought on plants is crucial for developing effective strategies to mitigate damage and enhance plant resilience and adaptation to these changing conditions.

To cope with drought, plants employ various strategies involving numerous biological mechanisms activated during different growth stages at the cellular, organ, and whole plant levels (Kumar et al., 2018). While plant responses to drought stress are intensively investigated from cellular to community levels (e.g., Kumar et al., 2018; Ploughe et al., 2019), plant drought responses at the metabolite level are still limited to investigating a few cellular processes (e.g., Almeida et al., 2020; Fàbregas & Fernie, 2019; You et al., 2019), and general metabolic profile changes are poorly understood. Metabolic profiles provide an understanding of whole cellular functioning and may thus help in developing strategies to enhance plant resilience to drought(Bowne et al., 2012; Calleja-Satrustegui et al., 2024). Untargeted metabolomics also

provides a broad, unbiased view of metabolic shifts, allowing identification of novel metabolites and pathways that may be involved in drought responses.

Most research on the drought effects on plants looks at the responses to single drought events (e.g., Gupta et al., 2020; Ploughe et al., 2019), and far less attention has been given to how plants cope with recurrent drought episodes (but see e.g., Virlouvet & Fromm, 2015; Kambona et al., 2023). Understanding the effect of recurrent drought is, however, becoming increasingly important as drought events are becoming more frequent (IPCC 2023), requiring plants to not just survive individual stress events but also develop adaptive strategies to deal with repeated drought via stress memory (Crisp et al., 2016).

Stress memory involves structural changes, epigenetic reprogramming, and biochemical adjustments during initial drought exposure, priming plants for more efficient future responses through sustained gene expression changes, protective protein accumulation, and ongoing metabolic reprogramming (Crisp et al., 2016; Fleta-Soriano & Munné-Bosch, 2016; Sharma et al., 2022). Exploring metabolic changes linked to stress memory may broaden our understanding of how plants adapt to environmental challenges by identifying key metabolites, revealing diverse cellular pathways and structural responses involved in long term stress adaptation (Aina et al., 2024). Studying the metabolic changes will thus help us to understand how plants 'remember' stress at the molecular level and reorganize their metabolome to become more resilient to recurrent drought. Even stronger inferences can be made by linking the metabolic changes to morphophysiological changes in the same individuals(Walker et al., 2023), but such comparisons are extremely rare.

Plant hormones play a crucial role in modifying plant performance under drought conditions (Salvi et al., 2021a; Waadt et al., 2022). Methyl jasmonate (MeJA) enhances plant resilience to drought by regulating key developmental processes such as seed germination, root

growth, flowering, and senescence (Hewedy, Elsheery, Karkour, Elhamouly, Arafa, Mahmoud, Dawood, Hussein, Mansour, Amin, et al., 2023; Yu et al., 2018). It also influences root and shoot growth, promoting water uptake and plant health during drought (Lee & Zwiazek, 2019; Wei et al., 2025). Despite growing evidence for MeJA's effectiveness in enhancing drought tolerance(Balbontín et al., 2024; Đurić et al., 2024; Khan et al., 2024; Wei et al., 2024), its potential to induce transgenerational stress memory carried through metabolic or epigenetic changes remains largely unexplored.

This study uniquely combines untargeted metabolomics with morpho-physiological analyses to investigate whether MeJA priming imprints a stress memory that benefits subsequent generations under recurrent drought conditions. It further explores the role of drought induced memory and how MeJA and drought related memory interact to shape plant performance under water stress. At the metabolomic level, we assessed changes in metabolite diversity and composition of the entire metabolome. At the morpho-physiological level, we evaluated specific leaf area, relative water content, leaf dry matter content, chlorophyll content, and chlorophyll fluorescence. Finally, we investigated whether metabolomic profiles and plant morpho-physiology are related, revealing predictive power from each other and indicating integrated, memory driven strategies for enhanced stress resilience. We used *F. rubra*, a dominant grass species of alpine grasslands, as a model. Thanks to its frequent vegetative reproduction, this species is a perfect model for studying the transmission of stress memory among clonal generations.

We hypothesize the following: **H1** – Exposure to current drought (D2) strongly influence the metabolomic and morpho-physiological traits of *F. rubra*, representing immediate stress induced changes. **H2**-Prior exposure to drought (D1) and methyl jasmonate (MeJA, M1) induces transgenerational memory in clonal offspring, leading to persistent reprogramming of the metabolome and modulation of key morpho-physiological traits such as specific leaf area

(SLA), relative water content (RWC), and chlorophyll dynamics thereby enhancing plant responses to recurrent drought stress even in the absence of current drought. **H3** – Drought and methyl jasmonate memories will interact with current drought such that combinations of past and present stress exposures will produce synergistic or compensatory effects on plant metabolome and morpho-physiology. **H4**- Finally, we hypothesize that metabolomic profiles and morphophysiological traits are tightly linked, reflecting coordinated memory-driven responses across molecular and phenotypic levels that enhance drought resilience.

2. Materials and Methods

2.1 Study system

We used ramets of *F. rubra* from our previous experiment (Bhatt et al. subm.) for this study. The previous experiment involved a factorial combination of drought (yes/no) and MeJA (yes/no) treatments and 10 replicates per treatment. *F. rubra* ramets were grown in pots with natural grassland soil under controlled conditions. Drought stress was applied in two phases, with recovery phases in between, while MeJA was applied to the soil during drought phases and not during the recovery phases. Control plants received regular watering. The MeJA soil application was chosen to ensure consistent distribution and minimize environmental loss. More details from the previous experiment are given in (Text S1).

In this experiment, ramets previously subjected to different drought and MeJA treatments (referred to as parental treatment) were grown in pots containing soil exposed to either drought or MeJA + drought in the previous experiment. Six replicates of ramets from the four parental treatments were grown in each soil with different memories (i.e., 2 parental drought treatments × 2 parental MeJA treatments × 2 soil memories × 2 current drought × 6 replicates). Although soil memory (SM) was included in the experimental design to account for potential legacy effects from the previous generation, it was not a primary focus of this

study. SM showed statistically significant effects only in the metabolomic composition analyses and was not significant in any other aspect of the study. Consequently, SM is not presented in the main text, and its results are presented only in (Table S1). We focus only on intrinsic plant memory mechanisms, specifically current drought (D2), drought memory (D1), and MeJA memory (M1).

Three of these replicates were well watered, and the remaining three were subjected to recurrent drought cycles followed by recovery phases. This included 30 day cycles of drought and recovery (Drought stage 1 - Recovery stage 1 - Drought stage 2 - Recovery stage 2). No MeJA treatment was applied, as the focus was on investigating the legacy effects of prior MeJA treatment on the metabolome of next-generation ramets under recurrent drought conditions.

The plants were grown in 200 ml pots. One *F. rubra* ramet was planted into each pot. All planted ramets were of similar age and size (3 weeks old, 3.5-4 cm tall). They were grown under long-day conditions (16 hours of daylight) in a growth chamber (17–20 °C Day and 7–10 °C Night), reflecting peak growing season conditions at the original locality. The plants were allowed to establish for 21 days before starting the experiment.

2.2 Plant performance

Plant physiology was characterized by chlorophyll content, chlorophyll fluorescence (Fv/Fm), specific leaf area (SLA), leaf dry matter content (LDMC), and leaf relative water content (RWC). These traits provide critical information about how plants structurally and physiologically adapt to drought stress(Maxwell & Johnson, 2000; Perez-Harguindeguy et al., 2013a).

Chlorophyll content and Chlorophyll fluorescence (Fv/Fm) were measured at the end of each stress and recovery phase. SLA, LDMC, and RWC were measured only once, at the

end of the second recovery phase, due to their destructive nature, which prevented repeated measurements.

2.2.1 Chlorophyll Content and Chlorophyll Fluorescence

Chlorophyll is an essential pigment crucial for photosynthesis, and its detection in plants is a significant indicator of their chlorophyll fluorescence and overall well-being (Muller et al., 2011). In our study, we utilized a chlorophyll CCM 300 meter to quantify the chlorophyll content in plant leaves. Three randomly selected leaves were chosen from each pot, and the chlorophyll content was measured according to the instructions provided by the manufacturer once per leaf. The mean of these 3 values has been used as the dependent variable in the subsequent analyses.

Chlorophyll degradation can decrease the maximum efficiency of Photosystem II (PSII) known as the Fv/Fm ratios, decreasing the net photosynthetic rate (Chungloo et al., 2023). Photon System Instrument FluorPen FP-100 MAX determined the chlorophyll fluorescence of PSII. Healthy plants adapted to darkness have chlorophyll fluorescence ratios ranging from 0.75 to 0.85 (Björkman & Demmig, 1987). Lower values indicate damage to the system. chlorophyll fluorescence was measured in the afternoon, and a 1-hour dark acclimation was achieved by using the manufacturer provided clips. Chlorophyll content and chlorophyll fluorescence were measured across four key phases: stress phase 1, recovery phase 1, stress phase 2, and recovery phase 2. Based on the correlation analysis (Figure S1), two representative variables were selected to reduce redundancy and multicollinearity: CCS2 (Chlorophyll Content during Stress Phase 2) and CFR1 (Chlorophyll Fluorescence during Recovery Phase 1).

CCS2 showed strong correlations ($r \geq 0.7$) with other chlorophyll content traits from stress phase 2 and both recovery phases, as well as with chlorophyll fluorescence traits from

both stress phases. This suggests that CCS2 effectively captures broader chlorophyll related variation across phases. Similarly, CFR1 was highly correlated with CFR2 (Chlorophyll Fluorescence during Recovery Phase 2), making it a suitable representative of the recovery-phase fluorescence response.

2.2.2 SLA, LDMC, and RWC

SLA (Specific leaf area) and LDMC (Leaf dry matter content) are frequently used to predict drought resistance because they essentially represent a trade-off between conservation and rapid resource uptake (Blumenthal et al., 2020; Perez-Harguindeguy et al., 2013b). RWC (Relative water content) serves as the most appropriate measure for assessing a plant's water status, providing insight into cellular water deficit and the impact of Osmotic Adjustment on maintaining cellular hydration during drought stress (Barrs & Weatherley, 1962).

Due to the extremely narrow and naturally folded morphology of *F. rubra* leaves, accurately determining leaf area from scanned images proved unreliable. To standardize measurements, we selected approximately 4 cm-long segments from individual leaves per pot. Fresh weight was recorded for each segment. Because the leaves could not be fully unfolded without damage, we measured both the length and width of each segment using a magnifying glass. Leaf area was then estimated using the formula: length × width × 2, accounting for the folding of the leaf blade. Subsequently, the leaf segment was placed in a Petri plate filled with water overnight in a refrigerator to rehydrate. After the leaves had been rehydrated, any extra water on the surface was carefully removed, and the leaves were weighed to determine their turgid weight. The leaves were then dried in a 65°C oven for two days to determine their dry weight. Using these measurements, we calculated the SLA by determining the ratio of leaf area (mm^2) to dry mass (mg), LDMC by dividing the dry leaf mass (mg) by the turgid mass (g), and

Relative water content RWC as RWC (%) = [(Fresh weight - Dry weight) / (Turgid weight – Dry weight)] x 100.

2.2.3 **Metabolite Profiling**

2.2.3.1 Plant sampling

Samples were collected at the end of the second drought phase. Approximately 20 leaves per individual from multiple ramets per individual were sampled and pooled. Leaves were carefully excised using sterile scissors, then wrapped in aluminium foil and immediately placed in liquid nitrogen for snap freezing and temporary storage. After sampling all the plants, the samples stored in liquid nitrogen were transferred to a -80°C freezer for storage until further analyses.

2.2.3.2 Methanol extraction

We took ~100 mg of each sample. We placed it into 1.5 ml microcentrifuge tubes (MCT) containing 3 metal beads and 500 µL of an extraction solvent composed of methanol and water (80:20). The samples were homogenized using a homogenizer. After homogenization, samples were thoroughly vortexed for 10 seconds, followed by a 24-hour incubation at -20 °C. After incubation, the tubes were vortexed again and centrifuged at 13000 rpm for 15 minutes. The supernatant was carefully transferred into new tubes. The same steps of the extraction process, from adding the solvent, were repeated once to ensure complete metabolite extraction. The supernatants from both extraction rounds were pooled together. From this combined pool, 320 µL was transferred to a new tube, and 80 µL of a water/formic acid solution (99.9/0.1 v/v, respectively) was added to the tube. The samples were then stored at -20 °C for at least 48 hours. Three blanks were processed alongside the samples to detect solvent-related contamination, following all extraction steps but excluding leaf tissue. Additionally, quality controls were created by pooling 20 µL from each sample extract.

2.2.3.3 Liquid Chromatography Data Acquisition

218 Chromatographic separation was performed at 40 °C using a 6546 LC/Q-TOF (Agilent) system
219 equipped with an Acclaim® RSLC 120 column (150 × 2.1 mm, 2.2 µm particle size; Thermo
220 Fisher Scientific). The chromatographic run began with an initial mobile-phase composition
221 of 95 % A, maintained for the first 3 minutes. From 0–3 minutes, the proportion of A was
222 linearly reduced to 82.7 %, then decreased to 76 % by the 10-minute mark. A steep linear
223 gradient followed between 10 and 17 minutes, dropping sharply from 76 % to 5 %, which was
224 held constant for one minute. A rapid re-equilibration occurred between 18 and 18.1 minutes,
225 raising A back to 95 %, and this composition was maintained through 20 minutes. The entire
226 sequence was executed for both positive and negative ionization modes. MS/MS analysis was
227 also performed in the same settings in a data-dependent mode, with 4 analyses conducted from
228 QC samples.

229 *2.3.3.4 Spectral processing*

230 Spectral processing of the LC-MS data was performed to extract relevant features for
231 metabolite identification and quantification. The raw data, which contained metabolites and
232 their concentrations across multiple time points, was processed using the MetaboAnalystR
233 Package of R (Pang et al., 2024). Several preprocessing steps were further applied to ensure
234 the quality and reliability of the acquired data. First, data were filtered to remove features with
235 more than 85% missing values, which helps eliminate unreliable or incomplete data. Missing
236 values were then imputed using the $1/5^{th}$ of the lowest value (Pang et al., 2024). This step is
237 essential to minimize the impact of missing values, which may arise due to biological
238 variability or technical limitations in detection sensitivity. Subsequently, the data were quantile
239 normalized, log transformed and scaled to stabilize variance and ensure comparable
240 distributions across samples. However, for estimating metabolite diversity metrics (richness,
241 Shannon diversity, and evenness), the processed data were deemed unsuitable due to
242 transformations that alter the original distribution of metabolite presence. Therefore, diversity

243 estimates were calculated using the unprocessed data to preserve the integrity of presence-
244 absence and abundance patterns.

245 **2.3 Data analysis**

246 All the metabolome analyses have been done separately for positive and negative ionization
247 modes as in previous studies (e.g. Calderón-Santiago et al., 2016; Nordström et al., 2008; Tian
248 et al., 2013).

249 *2.3.1 Metabolite diversity and Uniqueness*

250 To evaluate the effects of transgenerational memory of drought and Methyl Jasmonate (MeJA)
251 on metabolite diversity, we analyzed three key diversity indices, i.e., metabolite richness,
252 Shannon diversity, and Hill evenness (HillEven). Richness was estimated as the total number
253 of detected metabolites in each of the samples. Shannon diversity and HillEven were estimated
254 using the Chemodiv Package of R (Petrén et al., 2023). These indices were chosen because
255 they provide complementary insights into the metabolome: Shannon diversity captures both
256 the number and relative abundance of metabolites, reflecting metabolic complexity, while Hill
257 evenness quantifies how evenly metabolite abundances are distributed, which is critical for
258 understanding dominance patterns in untargeted metabolomics datasets. Additionally,
259 metabolomic uniqueness was evaluated by calculating the average Euclidean distance of each
260 sample from all others based on standardized metabolite intensities (Ren et al., 2015) .

261 Linear models were fitted using a full factorial design incorporating all treatments: D1, D2,
262 M1, and their two-way interactions. Before analyses, Richness, Shannon Diversity, and Hill
263 Evenness were log-transformed to fulfil the data normality assumption. Because the results of
264 Hill evenness largely matched the results of Shannon diversity in our analyses ($r = 0.96$), they
265 are not reported further. They are only shown in supporting information (Table S2 and Figure
266 S2, S3).

267 *2.3.2 Multivariate analyses*

268 Multivariate analyses were applied to examine the interactive effects of treatments and morpho-
269 physiological traits on the metabolomic composition. Redundancy Analysis (RDA) as
270 implemented in the vegan package in R was used throughout to explore these relationships,
271 using standardized data for all dependent variables (i.e., metabolites). A full model including
272 all main effects of D1, D2, M1, and their interactions was constructed. The significance of each
273 predictor was determined using permutation tests (n = 999), and variance partitioning was used
274 to quantify their contribution to overall variation. A similar RDA approach was used to
275 investigate how morpho-physiological traits influence metabolomic composition and how the
276 treatments affected plant morpho-physiological traits.

277 *2.3.3 Effect of treatments on each metabolite*

278 To visualize the overlap and specificity of metabolite responses across treatment groups, we
279 quantified the number of significantly affected metabolites (FDR-adjusted $p < 0.05$) for each
280 main effect (D1, M1, D2) and their pairwise interactions (D1×D2, D1×M1, D2×M1).
281 Significant metabolites were extracted from the linear model output, and treatment-specific
282 metabolite sets were defined. A binary presence/absence matrix was constructed across all
283 groups, enabling classification of each metabolite as either unique (significant in one group
284 only) or shared (significant in multiple groups). The resulting counts were visualized using bar
285 plots in R (version 4.2.1). To visualize changes in metabolite content, a heatmap was
286 constructed based on group-level averages of significant metabolites, with hierarchical
287 clustering. Also, due to the huge number of significant metabolites, only the top 100 were used
288 in the heatmap.

289 *2.3.4 Annotation of significantly affected metabolites*

We annotated the metabolites significantly affected by climate. For this, data-dependent LC-MS/MS analysis was performed on a pooled sample (used as a quality control in LC-MS analysis) to collect the necessary data. Subsequently, we used MS-DIAL (Tsugawa et al., 2015) software to putatively annotate the metabolites detected in LC-MS/MS mode data. LC-MS/MS data was processed by aligning retention times, detecting peaks, and deconvoluting spectra. The annotation was then done by matching detected compounds against freely available libraries at https://systemsomicslab.github.io/compms/msdial/main.html. A mass accuracy threshold of 10 ppm was used in the annotation process. After annotation, the metabolites were assigned to their chemical classes.

3 Results

3.1 Metabolite Diversity

The effect of current drought (D2) and its interaction with drought memory (D1) was statistically significant (Table 1) in the positive ionization mode. Metabolite richness declined under D2, indicating a narrowing of the metabolomic profile in response to stress. The significant interaction between D1 and D2 suggests that the benefits of drought memory on metabolomic diversification are conditional upon subsequent drought exposure. Specifically, drought memory (D1) increased metabolite richness under non stress conditions, but had the opposite effect under current drought, where richness was lowest in plants that had been previously exposed to drought (Figure 1a).

For Shannon diversity, both D1 and M1 had statistically significant effects in the positive ionization mode (Table 1), indicating that each memory treatment independently affects metabolite diversity. D1 individually caused a decline in Shannon diversity, while M1 caused an increase. Their interaction (D1 × M1) was also significant (Table 1), indicating that the effect of M1 on Shannon diversity depends on D1. Specifically, M1 caused an increase in Shannon diversity in the absence of D1 memory, but the combined presence of D1 and M1

memories shaped Shannon diversity by negating the effects of each other and bringing the Shannon diversity to control levels (both D1 and M1 are absent) (Figure 1b). In contrast, D2 did not significantly influence Shannon diversity in the positive mode but showed a strong effect in the negative ionization mode (Table 1), where it significantly decreased Shannon diversity, reflecting a more uneven distribution of metabolites under stress.

3.2 Metabolomic Uniqueness

The current drought (D2) was a significant predictor of metabolomic uniqueness in both positive and negative ionization modes (Table 1), while M1 and D1 were not. A significant interaction between D1 and D2 was also detected (Table 1), showing that metabolite uniqueness declined under D1 alone but increased notably when drought memory plants were exposed to current drought (Figure 1c). Also, the interaction between D2 and M1 was statistically significant (Table 1). Plants without MeJa memory without current drought showed the lowest uniqueness, plants without MeJa memory with current drought showed the highest uniqueness and plants with MeJa memory, independent of current drought being in between (Figure 1d). While the figures show results for the positive mode only, the results for the negative mode are largely similar (Figure S4 a)

The triple interaction (D1 × D2 × M1) was significant for metabolic uniqueness in negative mode. Plants with both drought and MeJa memory grown under drought exhibited the highest metabolic uniqueness compared to all the other treatments (Figure S5).

3.3 Determinants of metabolome composition

D2 was the strongest predictor of metabolome composition in both positive and negative ionization modes (Table 2). M1 and D1 (Table 2) also had significant and independent impacts on metabolite profiles in both modes, though their effects were comparatively lower than D2. The interactions D1×M1 and D2×M1 were also statistically significant (Table 2), indicating

339 that the combination of stress memory with current drought or between both memory types
340 altered metabolite composition. In contrast, the interaction between D1 and D2 did not show a
341 significant effect in either mode.

342 **3.4 Effect of MeJA memory and its interaction with drought on specific metabolites**

343 In the positive ionization mode, D2 induced the most significant metabolic changes, uniquely
344 affecting 475 metabolites and sharing 935 with other treatments, underscoring its central role
345 in metabolomic reprogramming (Figure S7a). M1 had the second largest impact, with 90
346 unique metabolites and 389 shared, while D1 had the smallest individual effect with 19 unique,
347 249 shared metabolites. Interaction terms also demonstrated pronounced metabolic responses.
348 The D2 × M1 interaction influenced the most metabolites among combinations (39 unique, 205
349 shared), followed by D1 × M1 (19 unique, 192 shared), while D1 × D2 showed minimal effect
350 (0 unique, 1 shared).

351 In the negative ionization mode (Figure S7b), D2 again triggered the strongest
352 metabolic shifts (462 unique, 952 shared), with M1 (73 unique, 396 shared) and D1 (30 unique,
353 311 shared) trailing behind. Similarly, interactions revealed substantial effects: D2 × M1 (54
354 unique, 170 shared), D1 × M1 (28 unique, 245 shared), and again, D1 × D2 (0 unique, 1 shared).

355 These findings highlight D2 as the primary driver of metabolic reprogramming, while
356 memory effects from M1 and D1 also shape distinct biochemical landscapes. The notably high
357 number of unique metabolites in D2 × M1 and D1 × M1 interactions indicates a non-additive,
358 context-dependent integration of stress memory with ongoing drought stress.

359 The heatmap of the top 200 differentially accumulated under different conditions and
360 annotated metabolites in both positive and negative mode (Figure 3). Clusters 1-4 in the
361 positive ion mode heatmap illustrate distinct metabolic strategies shaped by MeJA memory in
362 *F. rubra*. Cluster 1 metabolites, including phenolic compounds, flavonoids, curcuminoids,

363 saccharolipids, and linear diarylheptanoids, are upregulated in M1D2-treated plants, revealing
364 a jasmonic acid (JA) specific metabolic imprint, while D2, D1D2, and M1D1D2 treatments
365 show downregulation, suggesting that drought memory alone or in combination interferes with
366 this JA-associated response. Cluster 2 metabolites are selectively upregulated in both M1 and
367 M1D2, including alkaloids, terpenoids, isoflavonoids, lignans, and oligopeptides, indicating
368 that this set is a robust MeJA memory marker that does not require current stress for activation.
369 This exclusive response in MeJA primed plants makes Cluster 2 a clear biomarker for JA-
370 driven metabolic readiness. In contrast, Cluster 3 metabolites such as phosphocholines,
371 salicylamides, diacylglycerols, ether lipids, and flavonoid derivatives are selectively
372 downregulated only in M1 and M1D2, whereas all other treatments, regardless of memory,
373 show upregulation. This suggests that MeJA priming deliberately suppresses this non-primed,
374 general stress response pathway, likely to conserve energy and direct metabolism toward more
375 specialized defenses. Lastly, Cluster 4 is uniquely downregulated in M1D2, whereas D2,
376 D1D2, and M1D1D2 exhibit strong upregulation of their lipid and redox related metabolites
377 including ceramides (Cer_NDS, CerP), fatty alcohol esters, gamma amino acids, and
378 pyridoxines. This pattern indicates that MeJA memory strategically suppresses broad stress
379 induced metabolic activation in favor of targeted defense, reinforcing its role in refining and
380 focusing the plant's metabolic response under recurring drought conditions.

381 In negative ion mode, Cluster 1 is selectively upregulated in M1, and M1D2 includes
382 metabolites such as flavonoids, coumarins, limonoids, glycerophospholipids, oligosaccharides,
383 and rotanones, establishing it as a MeJA memory-specific metabolic signature. In contrast, D2,
384 D1D2, and M1D1D2 show clear suppression of this cluster, indicating that drought memory
385 alone or even in combination with MeJA fails to activate, and may actively repress, these
386 pathways. This underscores the specificity and strength of MeJA driven priming in shaping
387 targeted metabolic defense readiness. Conversely, Cluster 2 displays the opposite trend M1D2

exhibits strong downregulation of broad stress response metabolites such as alkaloids, phosphatidic acid, alpha and N-acyl amino acids, methoxyphenols, and dihexosylceramides, while D2, D1D2, and M1D1D2 show robust upregulation. This contrast highlights a MeJA memory induced suppression of diffuse metabolic activation, reinforcing a strategic shift in *F. rubra* toward focused, energy efficient defense responses during drought stress.

3.5 Relationship between plant morpho-physiological traits and metabolite profiles

The redundancy analysis (RDA) shows that SLA and RWC were the plant traits having the strongest effects on metabolite profiles under both positive and negative ionization modes (Table 3). Chlorophyll content (CCS2) also contributed to explaining metabolomic variation, but to a lesser extent and LDMC had no significant effect on metabolite patterns.

3.6 Determinants of plant morpho-physiological traits

The redundancy analysis (RDA) showed that M1 was the strongest predictor of morpho-physiological traits in *F. rubra,* followed by D2 and D1 (Table 2). The interaction between D2 and M1 was also statistically significant, while other interactions (D1×D2 and D1×M1) were not significant. The triple interaction between D1×D2×M1 was also significant (Table 2). This suggests that the way D1 affects dependence on M1 changes depending on whether the plants are experiencing drought (D2).

LDMC, RWC, and CCS2 increased with M1 and D2×M1, indicating positive associations with these treatments. In contrast, SLA pointed in the opposite direction, suggesting a likely trade-off under those same treatments. CFR1 shows a positive association with M1, as both vectors point in the same leftward direction on the RDA biplot. This suggests higher CFR1 values under M1 treatment (Figure 2).

4. Discussion

This study provides one of the first comprehensive multi-trait and metabolomic analyses of transgenerational plant memory in response to drought and methyl jasmonate (MeJA) priming and interactions among different memories. Using *F. rubra* as a clonal model system, it reveals how recurrent drought (D2), drought memory (D1), and MeJA memory (M1) individually and interactively modulate metabolomic diversity and composition, along with morpho-physiological traits. A key novelty lies in the demonstration that memory effects persist and influence not only morphological adjustments but also the plant's systemic metabolic reprogramming. The study uniquely identifies that memory effects are interaction dependent, revealing conditional metabolomic shifts shaped by environmental context. It also shows that MeJA memory can compensate for or stabilize drought induced metabolic alterations, suggesting a promising tool for enhancing resilience in clonal or perennial species. This work advances understanding of plant stress memory mechanisms, particularly highlighting metabolomic memory as a transgenerational trait. We also demonstrated plant responses at morpho-physiological levels and how strongly the metabolomic and morpho-physiological changes relate to each other.

4.1 Current drought (D2) is the most important factor affecting metabolomic profiles and morpho-physiology

Our results strongly support Hypothesis 1, demonstrating that current drought (D2) is the most influential factor affecting both the metabolomic architecture and morpho-physiological traits of *F. rubra*. This aligns with previous studies showing that plants facing acute water deficit rapidly engage systemic metabolic and structural adjustments to maintain cellular integrity and ensure survival (Fàbregas & Fernie, 2019; Gupta et al., 2020). However, our study extends this link to the whole metabolome, showing that cellular processes are strongly affected by drought.

A key finding is the reduced metabolite richness under current drought (D2) in positive ionization mode, suggesting a metabolic streamlining strategy. Rather than initiating a broad response, plants appear to conserve resources by prioritizing metabolites critical for drought tolerance, supporting the idea of targeted metabolic adjustment under stress. In contrast, the negative ionization mode showed stable richness but increased Shannon diversity, indicating a shift toward even metabolite distribution in negative mode. This pattern likely reflects the prioritization of compounds such as lipids, amino acids, phenolics, lactones, and terpenoids, which are metabolites known for their roles in membrane stability, antioxidant defense, osmoprotection, and signaling under drought (Bowne et al., 2012; Fàbregas & Fernie, 2019).

We also observed a marked increase in metabolite uniqueness under drought, suggesting individualized metabolic trajectories. This aligns with findings in *Arabidopsis thaliana* and maize, where genotypes and tissues exhibited distinct metabolic responses to drought (Lozano-Elena et al., 2022)highlighting metabolic plasticity as a key resilience mechanism.

Morpho-physiological traits also responded strongly to drought. Notably, specific leaf area (SLA) and relative water content (RWC) were closely associated with D2 conditions. A higher SLA under drought reflects a strategy to maximize light capture with reduced carbon cost, although it comes with trade-offs, namely, thinner leaves with lower water retention and photosynthetic capacity (Gonzalez-Paleo & Ravetta, 2018; Sun et al., 2025; Zhou et al., 2020).These changes underscore that drought resilience involves adjustments at both metabolomic and morpho-physiological levels.

4.2 Transgenerational memory reprograms plant metabolome and morpho-physiology

A key finding of our study is the context-dependent manner in which D1 and M1 affect metabolomic richness and Shannon diversity. Both D1 and M1 significantly increased

metabolite diversity under non-stressed conditions, reflecting a primed state where plants maintain a wider array of metabolites in anticipation of future drought stress. This aligns with earlier findings that priming via prior stress exposure or hormone signaling can enhance metabolic readiness and resilience(Hilker & Schmülling, 2019a; Liu et al., 2022a).

The independent effect of M1 uncovered in this study highlights its powerful role in transgenerational metabolomic and morpho-physiological reprogramming. Its effects on metabolomic composition and morpho-physiological traits were stronger than the effect of drought memory (D1). Importantly, M1 significantly enhanced metabolomic Shannon diversity without increasing richness. This suggests that M1 enhances not the quantity, but the balance and distribution of metabolites, possibly preparing the plant for a more versatile response to various stressors. This aligns with the known role of jasmonates in mediating systemic defense signaling and metabolic priming (Avramova, 2019). MeJA memory plants also maintained higher relative water content (RWC) and chlorophyll content under stress (CCS2), reflecting enhanced drought preparedness through improved water retention and photosynthetic integrity (Maxwell & Johnson, 2000; Qiu et al., 2020). To our knowledge, no previous study has explored MeJa memory in non-model, clonally reproducing species integrating untargeted metabolome profiling and morpho-physiology. By linking MeJA memory to stable changes in metabolic architecture and drought relevant traits, this work provides a novel framework for understanding non-genetic inheritance of stress resilience and offers practical insights for enhancing plant performance in increasingly unpredictable climates (Latzel & Münzbergová, 2018; Liu et al., 2022b).

Our study shows that drought memory (D1) alone maintained high metabolite richness, comparable to control plants, consistent with prior studies showing that stress primed plants often exhibit enhanced metabolic capacity due to epigenetic remodeling of stress responsive pathways (Nguyen et al., 2022). Drought memory (D1) also played a pivotal role in

483 reprogramming plant morpho-physiology. In D1 plants, we observed a marked increase in
484 specific leaf area (SLA), indicative of a shift toward a resource acquisitive strategy. This
485 morphological adjustment, however, was accompanied by lower relative water content (RWC)
486 and reduced leaf structural density, suggesting a trade-off between growth efficiency and water
487 conservation(Blumenthal et al., 2020; Pérez-Ramos et al., 2013). The fact that drought memory
488 (D1) triggers plant responses even in the absence of current drought suggests it acts as a priming
489 mechanism, keeping plants in a preconditioned state(Crisp et al., 2016; Fleta-Soriano &
490 Munné-Bosch, 2016). This form of anticipatory plasticity allows plants to respond more
491 quickly and efficiently when drought returns. In unpredictable environments, such stress
492 memory enhances survival by proactively shaping plant metabolism and morphology, rather
493 than relying solely on reactive responses(Liu et al., 2022b).

494 Crucially, drought memory (D1) not only influenced morpho-physiological traits and
495 metabolomic diversity but also altered metabolome composition, supporting the idea that plants
496 retain a biochemical memory of past stress(Sharma et al., 2022). This memory appears to guide
497 transgenerational metabolomic strategies, exerting effects on both structural and biochemical
498 components. While earlier studies have shown that drought stressed plants can transmit
499 morpho-physiological traits to clonal offspring(Hilker & Schmülling, 2019b; Kambona et al.,
500 2023b; Latzel & Münzbergová, 2018; Liu et al., 2022b), our study is the first to extend these
501 inherited traits to metabolic reprogramming, demonstrating that drought memory modulates
502 both structural and biochemical systems across generations.

503 **4.3 Interactive effects of MeJA memory, drought memory, and current drought shape**
504 **plant responses**

505 In line with H3, the different types of memory interacted with the current drought. Specifically,
506 drought memory (D1) increased metabolomic richness in plants not exposed to recurrent

507 drought (D2), and reduced it in plants exposed to current drought. This suggests that drought
508 memory is not expressed uniformly but is modulated by current environmental conditions.
509 Under recurrent drought, drought memory may streamline the metabolic response, focusing on
510 a core set of drought tolerance metabolites, thereby reducing overall richness. In contrast, in
511 the absence of current drought, drought memory appears to promote a broader metabolic
512 profile, possibly as a generalized preparedness strategy. This finding extends previous work in
513 *Leymus chinensis* and rice, which showed that drought memory alters physiological states
514 (Kambona et al., 2023b), by demonstrating that it also shapes whole metabolome richness in a
515 context-dependent manner.

516 Similarly, MeJA induced memory (M1) influenced metabolism through interactions
517 with D1 and D2, highlighting its context-sensitive regulatory role. These interactions reinforce
518 the idea that MeJA establishes a stable and heritable priming state, enhancing the plant's
519 capacity to respond to future stress. While MeJA is known to modulate antioxidant pathways,
520 secondary metabolism, and hormonal signaling (Chungloo et al., 2023; Hewedy, Elsheery,
521 Karkour, Elhamouly, Arafa, Mahmoud, Dawood, Hussein, Mansour, & Amin, 2023; Tayyab et
522 al., 2020; Yu et al., 2018), our study is the first to demonstrate that MeJA priming induces
523 transgenerational metabolic memory, affecting both metabolomic diversity and morpho-
524 physiological traits, as well as interactions with other types of memory.

525 The D1 × M1 interaction revealed that MeJA memory restored metabolomic diversity
526 in plants with drought memory to levels comparable to controls, suggesting a compensatory
527 mechanism. This implies that MeJA memory may reactivate or stabilize biosynthetic pathways
528 that are otherwise suppressed by drought memory. Such a capacity to "reset" the metabolic
529 state across generations positions MeJA priming as a promising strategy to mitigate the long-
530 term effects of drought, particularly in clonal and perennial species. While prior studies report

individual effects of memory in plants (Aswathi et al., 2025), the interaction among memory types is rarely studied (Aswathi et al., 2025; Kambona et al., 2023b).

Another key and novel finding of this study is a significant three way interaction between drought memory (D1), current drought (D2), and MeJA memory (M1), which strongly influenced metabolomic uniqueness. This interaction reveals that multiple stress memories do not act independently or additively, but instead interact in complex, emergent ways to shape the plant metabolome. The resulting metabolomic profiles were distinct and variable among all treatment groups, suggesting that plants integrate diverse stress legacies to generate unique, context-specific metabolic responses. To our knowledge, this is the first study to demonstrate such a three way interaction affecting the plant metabolome, highlighting a previously unrecognized layer of complexity in stress memory research. These findings underscore the importance of considering multi-factorial and transgenerational stress interactions when studying plant adaptation. Our results also point to the potential of leveraging combined priming strategies such as MeJA application alongside drought conditioning to enhance adaptive plasticity and biochemical resilience in clonal species under increasingly unpredictable environmental conditions.

4.4 Metabolome and physiology relate strongly to each other

In line with Hypothesis 4 (H4), we found that metabolomic profiles and morpho-physiological traits are tightly linked. Redundancy analysis demonstrated that SLA and RWC were the strongest predictors of metabolomic variation, followed by Chlorophyll Content (CCS2). These traits, which are key indicators of plant water use strategy and photosynthetic function(Barrs & Weatherley, 1962; Blumenthal et al., 2020; Maxwell & Johnson, 2000; Pérez-Ramos et al., 2013) explained substantial portions of the variation in both positive and negative ionization modes. The tight coupling between these physiological traits and metabolome composition

strongly supports the perception that plants coordinate biochemical and phenotypic traits to adapt to both current drought and stress memory.

Cluster heatmap analysis revealed distinct regulation patterns among memory treatments, showing how specific metabolite families support morpho-physiological resilience. In positive ionization mode, Cluster 1 (Figure S8a)—including phenolics, flavonoids, lipids, and curcuminoids—was strongly upregulated only in M1D2. These compounds, known for their antioxidant, membrane stabilizing, and osmoprotective roles (Almeida et al., 2020b; Fàbregas & Fernie, 2019; Falcone Ferreyra et al., 2012) , help maintain high relative water content (RWC) and reduce oxidative stress. This aligns with lower specific leaf area (SLA) and greater chlorophyll retention in MeJA memory plants, indicating efficient structural and biochemical defense. Cluster 2 (Figure S8b), enriched in alkaloids, lignans, oligopeptides, amino acids, and terpenoids, was activated in M1 and M1D2 signatures of jasmonate regulated metabolism that preemptively bolster stress tolerance via ROS scavenging, structural fortification, and signaling (Avramova, 2019; Khan et al., 2024; Yu et al., 2018) . In contrast, Clusters 3 and 4 (Figures S8c–d), upregulated in non-MeJA treatments (D2, D1D2, M1D1D2) but suppressed in M1D2, contained phosphocholines, salicylamides, ceramides, pyridoxines, and other broad stress related metabolites. These are energetically costly and potentially disruptive to specific JA responses; their repression in M1D2 suggests metabolic economy and response specificity (Crisp et al., 2016; Liu et al., 2022b; Salvi et al., 2021b; Sharma et al., 2022).

In negative ionization mode, Cluster 1 (Figure S8e), selectively upregulated in M1D2, comprised flavonoids, coumarins, phosphatidic acids, macrolides, and limonoids—key agents in membrane repair, antioxidative buffering, and defense mobilization (Chungloo et al., 2023; You et al., 2019; Zhang et al., 2023) . This activation strengthens the link between metabolomic priming and stable RWC and photosynthesis. Conversely, Cluster 2 (Figure S8f), with amino

acid derivatives, purines, lipid messengers, and phenylpropanes, was elevated in D2, D1D2, and M1D1D2 but repressed in M1D2, indicating avoidance of energetically expensive signaling in MeJA memory plants (Aswathi et al., 2025; Hilker & Schmülling, 2019b). Altogether, the data show that MeJA memory orchestrates the upregulation of protective metabolites and suppression of redundant or costly pathways, tightly linking metabolomic profiles with enhanced physiological outcomes highlighting the mechanistic basis of drought resilience in clonal plants (Aina et al., 2024; Balbontín et al., 2024).

5 Conclusion

Our study demonstrates that both drought memory and methyl jasmonate-induced memory play critical roles in shaping plant responses to current drought, not only through individual effects but also via complex interactions. We show for the first time that these memories influence whole metabolome diversity and uniqueness in a context-dependent and transgenerational manner. Drought memory appears to streamline metabolic responses under recurring drought, while methyl jasmonate induced memory fine tunes and stabilizes them, even compensating for the legacy of past stress. These memory driven adjustments extend beyond metabolism to influence morpho-physiological traits, enhancing water retention and structural resilience.

Importantly, our findings highlight that stress memory is not static but dynamically expressed depending on environmental context. The ability of methyl jasmonate induced memory to restore diversity and promote protective traits across generations underscores its potential as a biotechnological tool for enhancing resilience in clonally reproducing perennial species. Together, these insights advance our understanding of plant stress memory as a multi-layered, heritable system, offering promising avenues for developing crops and wild species better adapted to increasingly variable climates.

Conflict of interest: Nothing to declare

Acknowledgements: GAUK project number 171724 supported the study. It was also partly supported by GAČR 22-00761S, a long-term research development project no. RVO 67985939 of the Czech Academy of Sciences and institutional support for science and research of the Ministry of Education, Youth, and Sports of the Czech Republic.

Author contributions: TB, DT, and ZM conceptualized the study; TB, ZM, and DT did the experimental setup; NR and TB meticulously prepared the samples for UPLC analysis, while NR, DT, and JS optimized the UPLC-MS method; JS and TC performed UPLC-MS analysis; The raw data were processed to obtain metabolite feature data by TB, DT, and JS; TB carried out data analysis with the help of DT and ZM. TB led the writing, with in-depth editing and suggestions from DT and ZM; DT and ZM are the senior authors; All authors approved the submission and declare no conflict of interest.

References

Aina, O., Bakare, O. O., Fadaka, A. O., Keyster, M., & Klein, A. (2024). Plant biomarkers as early detection tools in stress management in food crops: a review. *Planta*, *259*(3), 60. https://doi.org/10.1007/s00425-024-04333-1

Almeida, T., Pinto, G., Correia, B., Gonçalves, S., Meijón, M., & Escandón, M. (2020a). In-depth analysis of the Quercus suber metabolome under drought stress and recovery reveals potential key metabolic players. *Plant Science*, *299*, 110606. https://doi.org/https://doi.org/10.1016/j.plantsci.2020.110606

Almeida, T., Pinto, G., Correia, B., Gonçalves, S., Meijón, M., & Escandón, M. (2020b). In-depth analysis of the Quercus suber metabolome under drought stress and recovery reveals potential key metabolic players. *Plant Science*, *299*, 110606. https://doi.org/https://doi.org/10.1016/j.plantsci.2020.110606

Aswathi, K. P. R., Ul-Allah, S., Puthur, J. T., Siddique, K. H. M., Frei, M., & Farooq, M. (2025). The Plant Mind: Unraveling Abiotic Stress Priming, Memory, and Adaptation. *Physiologia Plantarum*, *177*(4), e70372.

Avramova, Z. (2019). Defence-related priming and responses to recurring drought: Two manifestations of plant transcriptional memory mediated by the ABA and JA signalling pathways. *Plant, Cell & Environment*, *42*(3), 983–997.

Balbontín, C., Reyes, M., Yáñez, M. A., Parra-Palma, C., Morales-Quintana, L., & Ramos, P. (2024). Enhancing blueberry drought resilience: ABA and MeJA hormonal formulations

unveil water-saving strategies. *Horticulture, Environment, and Biotechnology*. https://doi.org/10.1007/s13580-024-00640-4

Barrs, H. D., & Weatherley, P. E. (1962). A re-examination of the relative turgidity technique for estimating water deficits in leaves. *Australian Journal of Biological Sciences*, *15*(3), 413–428.

Björkman, O., & Demmig, B. (1987). Photon yield of O 2 evolution and chlorophyll fluorescence characteristics at 77 K among vascular plants of diverse origins. *Planta*, *170*, 489–504.

Blumenthal, D. M., Mueller, K. E., Kray, J. A., Ocheltree, T. W., Augustine, D. J., & Wilcox, K. R. (2020). Traits link drought resistance with herbivore defence and plant economics in semi-arid grasslands: The central roles of phenology and leaf dry matter content. *Journal of Ecology*, *108*(6), 2336–2351.

Bowne, J. B., Erwin, T. A., Juttner, J., Schnurbusch, T., Langridge, P., Bacic, A., & Roessner, U. (2012). Drought responses of leaf tissues from wheat cultivars of differing drought tolerance at the metabolite level. *Molecular Plant*, *5*(2), 418–429.

Calderón-Santiago, M., Fernández-Peralbo, M. A., Priego-Capote, F., & Luque de Castro, M. D. (2016). MSCombine: a tool for merging untargeted metabolomic data from high-resolution mass spectrometry in the positive and negative ionization modes. *Metabolomics*, *12*(3), 43. https://doi.org/10.1007/s11306-016-0970-4

Calleja-Satrustegui, A., Echeverría, A., Ariz, I., Peralta de Andrés, J., & González, E. M. (2024). Unlocking nature's drought resilience: a focus on the parsimonious root phenotype and specialised root metabolism in wild Medicago populations. *Plant and Soil*, 1–17.

Chungloo, D., Tisarum, R., Sotesaritkul, T., Praseartkul, P., Himanshu, S. K., Datta, A., & Cha-um, S. (2023). Exogenous Foliar Application of Methyl Jasmonate Alleviates Water-Deficit Stress in Andrographis paniculata. *Journal of Soil Science and Plant Nutrition*. https://doi.org/10.1007/s42729-023-01414-0

Crisp, P. A., Ganguly, D., Eichten, S. R., Borevitz, J. O., & Pogson, B. J. (2016). Reconsidering plant memory: Intersections between stress recovery, RNA turnover, and epigenetics. *Science Advances*, *2*(2), e1501340.

Đurić, M., Motyka, V., Dobrev, P. I., Nedvěd, D., Pokorná, E., Subotić, A., Trifunović-Momčilov, M., & Milošević, S. (2024). Changes in the Endogenous Phytohormone Status of Drought-Stressed Impatiens walleriana Hook. f. Plants Treated with Methyl Jasmonate. *Journal of Plant Growth Regulation*, 1–18.

Fàbregas, N., & Fernie, A. R. (2019). The metabolic response to drought. *Journal of Experimental Botany*, *70*(4), 1077–1085. https://doi.org/10.1093/jxb/ery437

Falcone Ferreyra, M. L., Rius, S. P., & Casati, P. (2012). Flavonoids: biosynthesis, biological functions, and biotechnological applications. *Frontiers in Plant Science*, *3*, 222.

Fiehn, O. (2002). Metabolomics—the link between genotypes and phenotypes. *Functional Genomics*, 155–171.

Fleta-Soriano, E., & Munné-Bosch, S. (2016). Stress memory and the inevitable effects of drought: a physiological perspective. *Frontiers in Plant Science*, *7*, 143.

Gonzalez-Paleo, L., & Ravetta, D. A. (2018). Relationship between photosynthetic rate, water use and leaf structure in desert annual and perennial forbs differing in their growth. *Photosynthetica*, *56*(4), 1177–1187. https://doi.org/10.1007/s11099-018-0810-z

Gupta, A., Rico-Medina, A., & Caño-Delgado, A. I. (2020). The physiology of plant responses to drought. *Science*, *368*(6488), 266–269. https://doi.org/10.1126/science.aaz7614

Hewedy, O. A., Elsheery, N. I., Karkour, A. M., Elhamouly, N., Arafa, R. A., Mahmoud, G. A.-E., Dawood, M. F.-A., Hussein, W. E., Mansour, A., & Amin, D. H. (2023). Jasmonic acid regulates plant development and orchestrates stress response during tough times. *Environmental and Experimental Botany*, *208*, 105260.

Hewedy, O. A., Elsheery, N. I., Karkour, A. M., Elhamouly, N., Arafa, R. A., Mahmoud, G. A.-E., Dawood, M. F.-A., Hussein, W. E., Mansour, A., Amin, D. H., Allakhverdiev, S. I., Zivcak, M., & Brestic, M. (2023). Jasmonic acid regulates plant development and orchestrates stress response during tough times. *Environmental and Experimental Botany*, *208*, 105260. https://doi.org/https://doi.org/10.1016/j.envexpbot.2023.105260

Hilker, M., & Schmülling, T. (2019a). Stress priming, memory, and signalling in plants. *Plant, Cell & Environment*, *42*(3), 753–761. https://doi.org/https://doi.org/10.1111/pce.13526

Hilker, M., & Schmülling, T. (2019b). Stress priming, memory, and signalling in plants. In *Plant, Cell & Environment* (Vol. 42, Issue 3, pp. 753–761). Wiley Online Library.

Kambona, C. M., Koua, P. A., Léon, J., & Ballvora, A. (2023a). Stress memory and its regulation in plants experiencing recurrent drought conditions. *Theoretical and Applied Genetics*, *136*(2), 26.

Kambona, C. M., Koua, P. A., Léon, J., & Ballvora, A. (2023b). Stress memory and its regulation in plants experiencing recurrent drought conditions. *Theoretical and Applied Genetics*, *136*(2), 26. https://doi.org/10.1007/s00122-023-04313-1

Khan, V., Princi, Mubashshir, M., Umar, S., & Iqbal, N. (2024). Methyl Jasmonate and Pseudomonas fluorescens Synergistically Boost Antioxidative Defense, Secondary Metabolites, and Osmolyte Production to Enhance Drought Resilience in Mustard. *Journal of Plant Growth Regulation*. https://doi.org/10.1007/s00344-024-11310-1

Kumar, S., Sachdeva, S., Bhat, K. V, & Vats, S. (2018). Plant responses to drought stress: physiological, biochemical and molecular basis. *Biotic and Abiotic Stress Tolerance in Plants*, 1–25.

Latzel, V., & Münzbergová, Z. (2018). Anticipatory Behavior of the Clonal Plant Fragaria vesca. *Frontiers in Plant Science*, *9*. https://www.frontiersin.org/articles/10.3389/fpls.2018.01847

Lee, S. H., & Zwiazek, J. J. (2019). Regulation of water transport in Arabidopsis by methyl jasmonate. *Plant Physiology and Biochemistry*, *139*, 540–547. https://doi.org/https://doi.org/10.1016/j.plaphy.2019.04.023

Liu, H., Able, A. J., & Able, J. A. (2022a). Priming crops for the future: rewiring stress memory. *Trends in Plant Science*, *27*(7), 699–716. https://doi.org/https://doi.org/10.1016/j.tplants.2021.11.015

Liu, H., Able, A. J., & Able, J. A. (2022b). Priming crops for the future: rewiring stress memory. *Trends in Plant Science*, *27*(7), 699–716.

Lozano-Elena, F., Fàbregas, N., Coleto-Alcudia, V., & Caño-Delgado, A. I. (2022). Analysis of metabolic dynamics during drought stress in Arabidopsis plants. *Scientific Data*, *9*(1), 90. https://doi.org/10.1038/s41597-022-01161-4

Maxwell, K., & Johnson, G. N. (2000). Chlorophyll fluorescence—a practical guide. *Journal of Experimental Botany*, *51*(345), 659–668.

Michaletti, A., Naghavi, M. R., Toorchi, M., Zolla, L., & Rinalducci, S. (2018). Metabolomics and proteomics reveal drought-stress responses of leaf tissues from spring-wheat. *Scientific Reports*, *8*(1), 5710.

Nguyen, N. H., Vu, N. T., & Cheong, J.-J. (2022). Transcriptional stress memory and transgenerational inheritance of drought tolerance in plants. *International Journal of Molecular Sciences*, *23*(21), 12918.

Nordström, A., Want, E., Northen, T., Lehtiö, J., & Siuzdak, G. (2008). Multiple Ionization Mass Spectrometry Strategy Used To Reveal the Complexity of Metabolomics. *Analytical Chemistry*, *80*(2), 421–429. https://doi.org/10.1021/ac701982e

Pang, Z., Lu, Y., Zhou, G., Hui, F., Xu, L., Viau, C., Spigelman, A. F., MacDonald, P. E., Wishart, D. S., Li, S., & Xia, J. (2024). MetaboAnalyst 6.0: towards a unified platform for metabolomics data processing, analysis and interpretation. *Nucleic Acids Research*, *52*(W1), W398–W406. https://doi.org/10.1093/nar/gkae253

Perez-Harguindeguy, N., Diaz, S., Garnier, E., Lavorel, S., Poorter, H., Jaureguiberry, P., Bret-Harte, M. S., Cornwell, W. K., Craine, J. M., & Gurvich, D. E. (2013a). *New handbook for standardised measurement of plant functional traits worldwide. Aust. Bot. 61, 167–234.*

Perez-Harguindeguy, N., Diaz, S., Garnier, E., Lavorel, S., Poorter, H., Jaureguiberry, P., Bret-Harte, M. S., Cornwell, W. K., Craine, J. M., & Gurvich, D. E. (2013b). *New handbook for standardised measurement of plant functional traits worldwide. Aust. Bot. 61, 167–234.*

Pérez-Ramos, I. M., Volaire, F., Fattet, M., Blanchard, A., & Roumet, C. (2013). Tradeoffs between functional strategies for resource-use and drought-survival in Mediterranean rangeland species. *Environmental and Experimental Botany*, *87*, 126–136.

Petrén, H., Köllner, T. G., & Junker, R. R. (2023). Quantifying chemodiversity considering biochemical and structural properties of compounds with the R package chemodiv. *New Phytologist*, *237*(6), 2478–2492. https://doi.org/https://doi.org/10.1111/nph.18685

Ploughe, L. W., Jacobs, E. M., Frank, G. S., Greenler, S. M., Smith, M. D., & Dukes, J. S. (2019). Community Response to Extreme Drought (CRED): a framework for drought-induced shifts in plant–plant interactions. *New Phytologist*, *222*(1), 52–69.

Ren, S., Hinzman, A. A., Kang, E. L., Szczesniak, R. D., & Lu, L. J. (2015). Computational and statistical analysis of metabolomics data. *Metabolomics*, *11*(6), 1492–1513. https://doi.org/10.1007/s11306-015-0823-6

Salvi, P., Manna, M., Kaur, H., Thakur, T., Gandass, N., Bhatt, D., & Muthamilarasan, M. (2021a). Phytohormone signaling and crosstalk in regulating drought stress response in plants. *Plant Cell Reports*, *40*(8), 1305–1329. https://doi.org/10.1007/s00299-021-02683-8

Salvi, P., Manna, M., Kaur, H., Thakur, T., Gandass, N., Bhatt, D., & Muthamilarasan, M. (2021b). Phytohormone signaling and crosstalk in regulating drought stress response in plants. *Plant Cell Reports*, *40*, 1305–1329.

Sharma, M., Kumar, P., Verma, V., Sharma, R., Bhargava, B., & Irfan, M. (2022). Understanding plant stress memory response for abiotic stress resilience: Molecular insights and prospects. *Plant Physiology and Biochemistry*, *179*, 10–24. https://doi.org/https://doi.org/10.1016/j.plaphy.2022.03.004

Sun, D., Lei, Z., Carriquí, M., Zhang, Y., Liu, T., Wang, S., Song, K., Zhu, L., Zhang, W., & Zhang, Y. (2025). Reductions in mesophyll conductance under drought stress are influenced by increases in cell wall chelator-soluble pectin content and denser microfibril alignment in cotton. *Journal of Experimental Botany*, *76*(4), 1116–1130.

Tayyab, N., Naz, R., Yasmin, H., Nosheen, A., Keyani, R., Sajjad, M., Hassan, M. N., & Roberts, T. H. (2020). Combined seed and foliar pre-treatments with exogenous methyl jasmonate and salicylic acid mitigate drought-induced stress in maize. *PLOS ONE*, *15*(5), e0232269-. https://doi.org/10.1371/journal.pone.0232269

Tian, H., Bai, J., An, Z., Chen, Y., Zhang, R., He, J., Bi, X., Song, Y., & Abliz, Z. (2013). Plasma metabolome analysis by integrated ionization rapid-resolution liquid chromatography/tandem mass spectrometry. *Rapid Communications in Mass Spectrometry*, *27*(18), 2071–2080. https://doi.org/https://doi.org/10.1002/rcm.6666

Tsugawa, H., Cajka, T., Kind, T., Ma, Y., Higgins, B., Ikeda, K., Kanazawa, M., VanderGheynst, J., Fiehn, O., & Arita, M. (2015). MS-DIAL: data-independent MS/MS deconvolution for comprehensive metabolome analysis. *Nature Methods*, *12*(6), 523–526. https://doi.org/10.1038/nmeth.3393

Virlouvet, L., & Fromm, M. (2015). Physiological and transcriptional memory in guard cells during repetitive dehydration stress. *New Phytologist*, *205*(2), 596–607.

Waadt, R., Seller, C. A., Hsu, P.-K., Takahashi, Y., Munemasa, S., & Schroeder, J. I. (2022). Plant hormone regulation of abiotic stress responses. *Nature Reviews Molecular Cell Biology*, *23*(10), 680–694. https://doi.org/10.1038/s41580-022-00479-6

Walker, T. W. N., Schrodt, F., Allard, P.-M., Defossez, E., Jassey, V. E. J., Schuman, M. C., Alexander, J. M., Baines, O., Baldy, V., & Bardgett, R. D. (2023). Leaf metabolic traits

reveal hidden dimensions of plant form and function. *Science Advances*, *9*(35), eadi4029.

Wei, T., Gao, H., Yang, D., Zhu, G., Zhang, C., Wang, B., Jia, H., Zhang, C., & Guo, J. (2024). Effects of methyl jasmonate on physiological characteristics and drought resistance of alfalfa (Medicago sativa) and ryegrass (Lolium perenne l.). *Journal of Plant Growth Regulation*, 1–18.

Wei, T., Gao, H., Yang, D., Zhu, G., Zhang, C., Wang, B., Jia, H., Zhang, C., & Guo, J. (2025). Effects of Methyl Jasmonate on Physiological Characteristics and Drought Resistance of Alfalfa (Medicago sativa) and Ryegrass (Lolium perenne L.). *Journal of Plant Growth Regulation*, *44*(1), 335–352. https://doi.org/10.1007/s00344-024-11469-7

Wild, J., Kopecký, M., Macek, M., Šanda, M., Jankovec, J., & Haase, T. (2019). Climate at ecologically relevant scales: A new temperature and soil moisture logger for long-term microclimate measurement. *Agricultural and Forest Meteorology*, *268*, 40–47. https://doi.org/https://doi.org/10.1016/j.agrformet.2018.12.018

You, J., Zhang, Y., Liu, A., Li, D., Wang, X., Dossa, K., Zhou, R., Yu, J., Zhang, Y., Wang, L., & Zhang, X. (2019). Transcriptomic and metabolomic profiling of drought-tolerant and susceptible sesame genotypes in response to drought stress. *BMC Plant Biology*, *19*(1), 267. https://doi.org/10.1186/s12870-019-1880-1

Yu, X., Zhang, W., Zhang, Y., Zhang, X., Lang, D., & Zhang, X. (2018). The roles of methyl jasmonate to stress in plants. *Functional Plant Biology*, *46*(3), 197–212.

Zhang, D., Liu, Y., Yang, Z., Song, X., Ma, Y., Zhao, J., Wang, X., Liu, H., & Fan, L. (2023). Widely target metabolomics analysis of the differences in metabolites of licorice under drought stress. *Industrial Crops and Products*, *202*, 117071. https://doi.org/https://doi.org/10.1016/j.indcrop.2023.117071

Zhou, H., Zhou, G., He, Q., Zhou, L., Ji, Y., & Zhou, M. (2020). Environmental explanation of maize specific leaf area under varying water stress regimes. *Environmental and Experimental Botany*, *171*, 103932.

Treatment	Richness				Shannon				Uniqueness			
	Positive mode		Negative mode		Positive mode		Negative mode		Positive mode		Negative mode	
	P-value	Variation explained	P-value	Variation explained	P-value	Variation explained	P-value	Variation explained	P-value	Variation explained	P-value	Variation explained
D1	0.43	-	0.7	-	0.011	12.29	0.83	-	0.20	-	0.31	-
D2	<0.001	23.6	0.54	-	0.927	-	0.008	14.41	0.001	28.72	0.001	44.07
M1	0.146	-	0.39	-	0.009	12.82	0.24	-	0.25	-	0.094	-
D1×D2	0.038	6.59	0.001	21.34	0.343	-	0.14	-	0.023	5.44	0.014	5.88
D1×M1	0.659	-	0.85	-	0.049	6.63	0.36	-	0.094	-	0.097	-
D2×M1	0.77	-	0.7	-	0.528	-	0.9	-	0.001	11.93	0.02	4.78
D1×D2×M1	0.309	-	0.484	-	0.38	-	0.954	-	0.074	-	0.012	5.39

Table 1: Effects of D1, D2, M1, and their interactions on Richness, Shannon diversity, and Uniqueness in both positive and negative modes. The variation explained is shown for the significant predictors ($p < 0.05$).

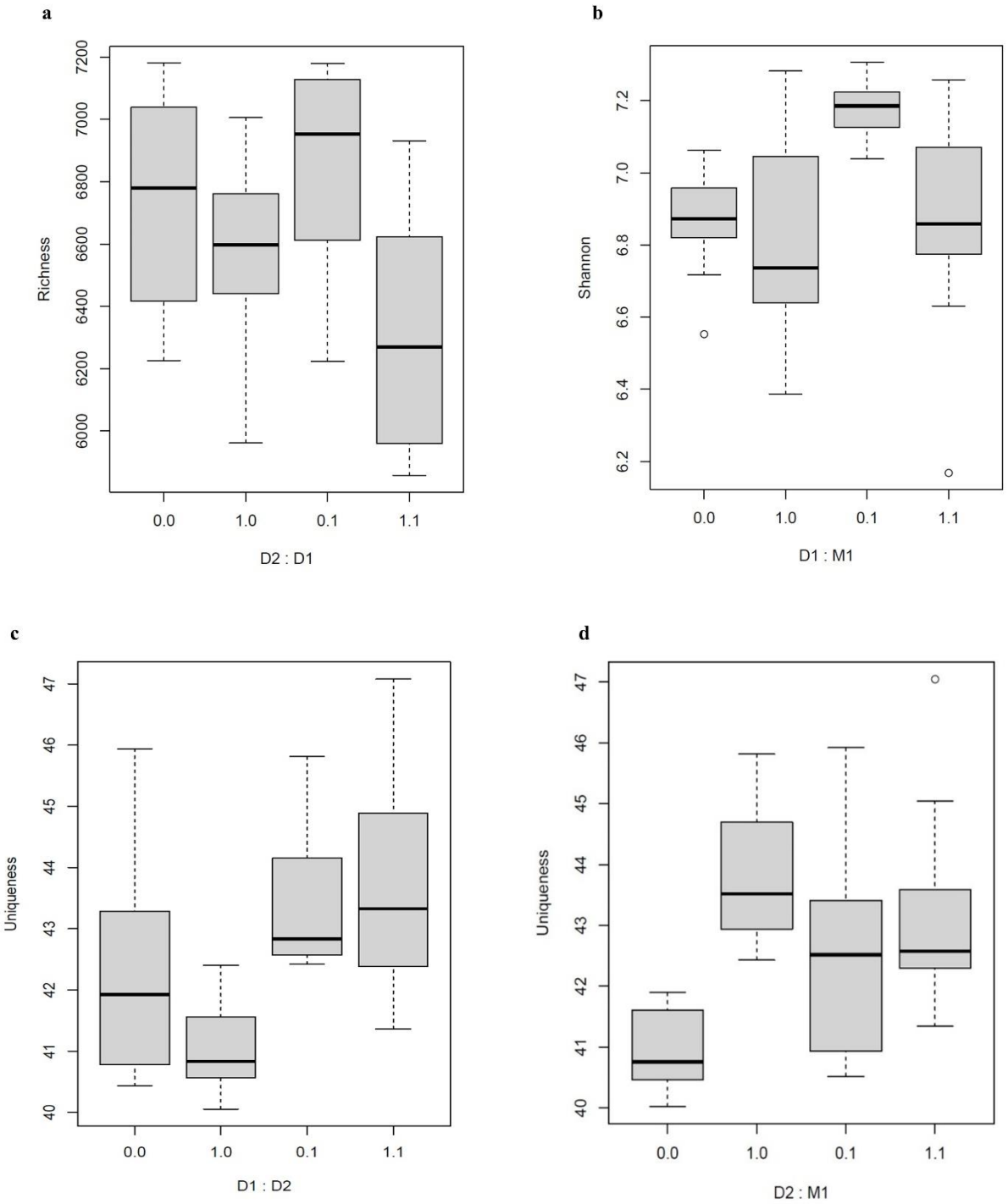

Figure 1: Boxplots showing the effects of interactions of D2, D1, and M1 in positive mode on metabolome (a) Richness, (b) Shannon diversity, and (c, d) Uniqueness in *F. rubra*. The X axis shows the levels of the interacting treatment, with 0 indicating absent and 1 present treatment (drought or MeJa).

Treatment	Metabolome				Physiology	
	Positive Mode		Negative Mode			
	p-value	Var. expl (%)	p-value	Var. expl (%)	p-value	Var. expl (%)
D1	0.004	3.51	0.001	4.14	0.001	18.34
D2	0.001	15.82	0.001	15.57	0.001	23.90
M1	0.001	5.16	0.001	4.92	0.001	31.12
D1×D2	0.151	-	0.098	-	0.146	-
D1×M1	0.005	3.7	0.001	3.66	0.158	-
D2×M1	0.002	3.5	0.004	3.49	0.001	9.83
D1×D2×M1	0.264		0.182		0.014	1.8

Table 2: Summary of Redundancy Analysis (RDA) results showing the effects of drought memory (D1), current drought (D2), MeJA memory (M1), and their interactions on metabolomic profiles (in positive and negative ionization modes) and morpho-physiological traits. The table reports the p-values and percentage of variation explained for each significant predictor. Only significant values ($p \leq 0.05$) are associated with variation explained (%); dashes (–) indicate non-significance.

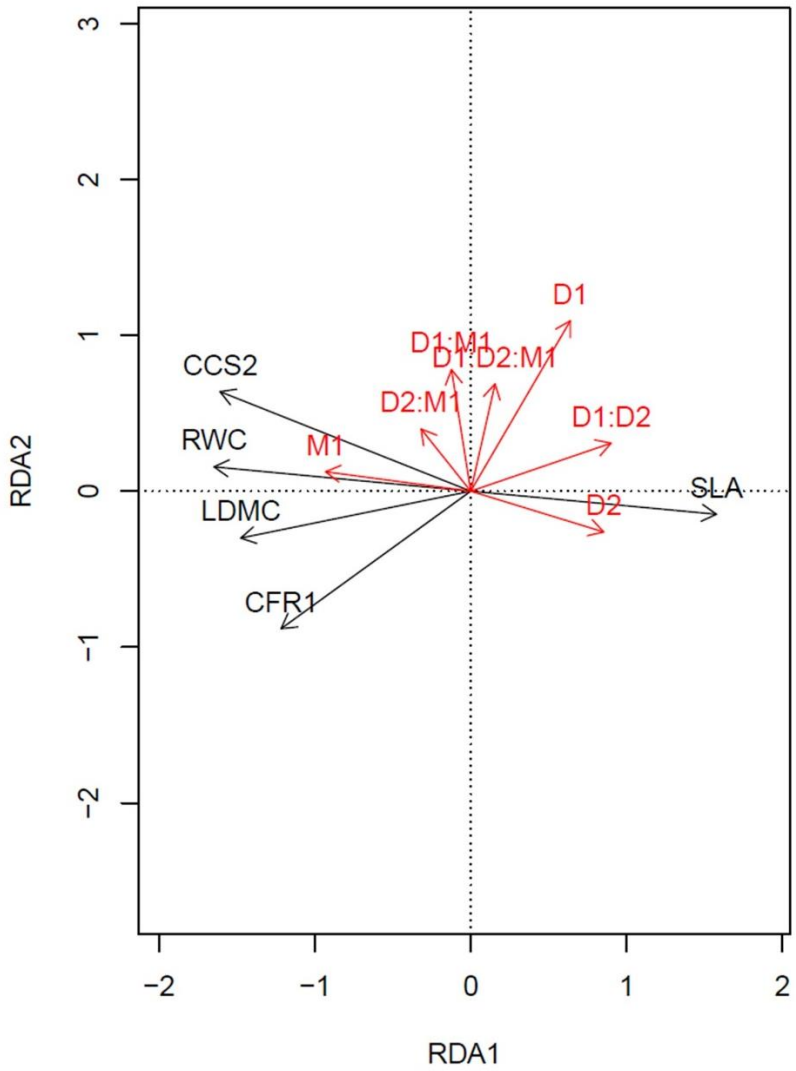

Figure 2: RDA biplot illustrating the relationships between treatment variables (shown as red arrows) and morpho-physiological traits (shown as grey arrows) in *F. rubra.*

	Positive mode		Negative mode	
	P	Var. expl (%)	P	Var. expl (%)
SLA	0.001	12.26	0.001	11.11
LDMC	0.112	-	0.106	-
RWC	0.003	4.18	0.001	4.07
CCS2	0.015	3.32	0.016	2.92
CFR1	0.135	-	0.136	-

Table 3: Effects on plant traits on metabolic composition for positive and negative ionization modes assessed using redundancy analysis (RDA).

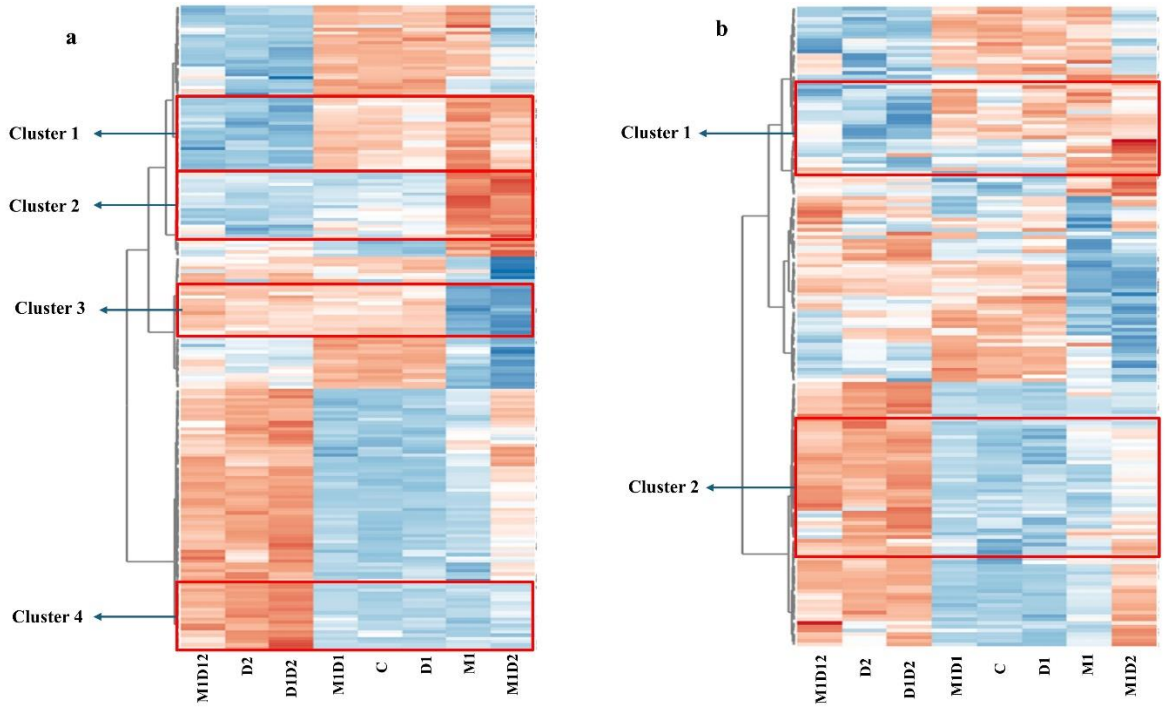

Figure 3: Heatmap displaying the scaled intensity values of differentially accumulated metabolites across various treatment groups in *F. rubra* (M1, D1, D2, i.e. MeJA memory, drought memory and current drought respectively), others are the plants which got combination M1, D2 and D2 treatment, while missing code in combination indicates that plants where not treated by the given treatment. C indicates Control, i.e., no drought or MeJa treatment memory, and also in well-watered conditions in both positive mode (a) and negative mode (b). The clustering was performed using hierarchical clustering based on Euclidean distance and complete linkage. The columns represent plants with different memory and current stress conditions. The orange color in the plot represents a higher accumulation of a metabolite, while the blue color represents a lower accumulation. Also, the zoomed image of marked clusters is provided in the supplementary material with upregulated and downregulated metabolite names in marked clusters.

Supplementary

Treatment	Richness (p-value)		Shannon (p-value)		Hill Even (p-value)		Uniqueness (p-value)		Metabolites-Treatment (p-value)		Traits-Treatment (p-value)
	P	N	P	N	P	N	P	N	P	N	
SM	0.077	0.118	0.45	0.77	0.63	0.67	0.073	0.038	**0.025**	**0.041**	0.131

Table S1: This table presents *p*-values comparing metabolome diversity metrics and metabolomic/trait-level responses for soil memory (SM). Metabolome analysis was performed in both positive (P) and negative (N) ionization modes. Significant results ($p < 0.05$) indicate treatment-induced effects and are in bold.

Text S2: **Experimental design**

The experiment represented a factorial cross of drought and MeJA treatments, each with two levels (yes/no). Each treatment had 10 replicates. The soil utilized in the experiment was sourced from the same meadow where the experimental plants were originally collected. Pots with a volume of 500 ml were filled with the soil, and one *F. rubra* ramet was planted into each pot. All the planted ramets were of similar age and size (approximately 3 weeks old and 3.5 to 4 cm tall). The plants were placed in a growth chamber with long-day conditions, where the temperature ranged from 17 to 20 °C during the day (16 hours) and 7 to 10 °C at night (8 hours). These conditions reflect conditions at the original locality during peak growing season. The plants were allowed to establish for 21 days before starting the experiment. The experiment included cycles of drought and recovery phases, each lasting 30 days (Drought stage 1 - Recovery stage 1 - Drought stage 2 - Recovery stage 2 - Drought stage 3 - Recovery stage 3).

Control watering treatment received regular watering daily, maintaining 1 cm of water above the pot base in the trays throughout the experiment. Drought-stressed plants received 50 ml of water in specific watering intervals during the drought stages: every 7th day during drought stage 1, every 10th day in drought stage 2, and every 15th day in drought stage 3. There was a progressive increase in drought stress among phases because treating plants to an excessive amount of stress initially can result in total plant loss, forcing the experiment to terminate after the first drought stage. In each phase, we attempted to expose the plants to as intense drought stress as possible but made sure they would survive successive drought stages. During the recovery stage, drought-stressed plants received the same watering as the control ones. The soil moisture has been monitored using TMS dataloggers (Wild et al., 2019).MeJA-treated *F. rubra* plants received 5 ml of 10 µM MeJA by pouring it directly onto the soil every 24 hours during the stress phases, but not during recovery. Only drought plants also got 5 ml of distilled water when 5 ml of 10 µM MeJA was given to MeJA-treated plants during drought. Previous studies

predominantly relied on foliar application of MeJA for plant treatment (e.g. Tayyab et al., 2020; Chungloo et al., 2023)We decided to apply it to the soil as foliar application has various disadvantages. The volatile nature of MeJA poses a risk of environmental loss when applied through foliar application, and there is an additional concern of uneven MeJA distribution among leaves across the plant. Therefore, soil application is a viable solution to address these challenges effectively. Soil is an efficient absorber, thus minimizing the risk of MeJA loss to the environment, while root uptake guarantees a more consistent distribution of MeJA throughout the entire plant.

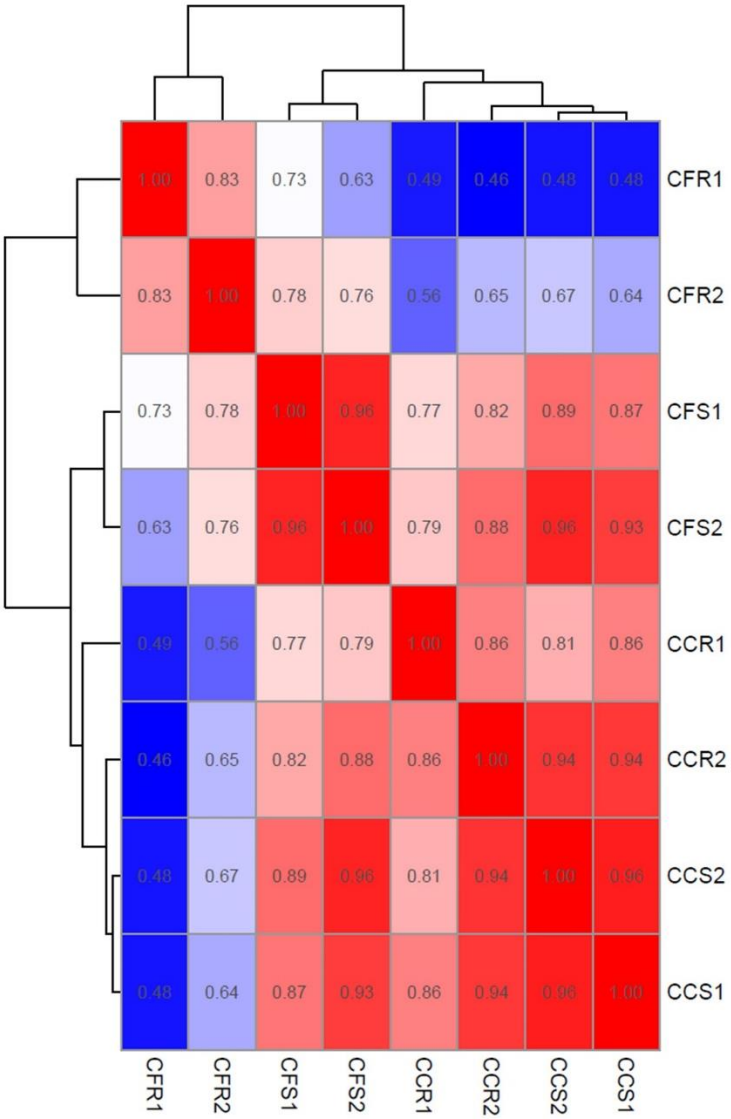

Figure S1: Correlation heatmap showing the relationship among chlorophyll fluorescence parameters measured during the stress phase (CFS1, CFS2), recovery phase (CFR1, CFR2), chlorophyll content measured during the stress phase (CCS1, CCS2), and recovery phase (CCR1, CCR2). Correlation coefficients are color-coded from dark blue (low correlation) to dark red (high correlation), with values displayed within each cell.

Treatment	Hill Eveness			
	Positive mode		Negative mode	
	P-value	Variation explained	P-value	Variation explained
D1	0.01	10.66	0.97	-
D2	0.357	-	0.01	14.35
M1	0.007	19.78	0.37	-
D1×D2	0.8	-	0.43	-
D1×M1	0.011	10.47	0.36	-
D2×M1	0.489	-	0.89	-
D1×D2×M1	0.167	-	0.897	-

Table S2: Table showing effects of M1, D1, D2, i.e., MeJA memory, drought memory, and current drought respectively, and their interactions on Hill Eveness. The variation explained is shown for the significant predictors ($p < 0.05$).

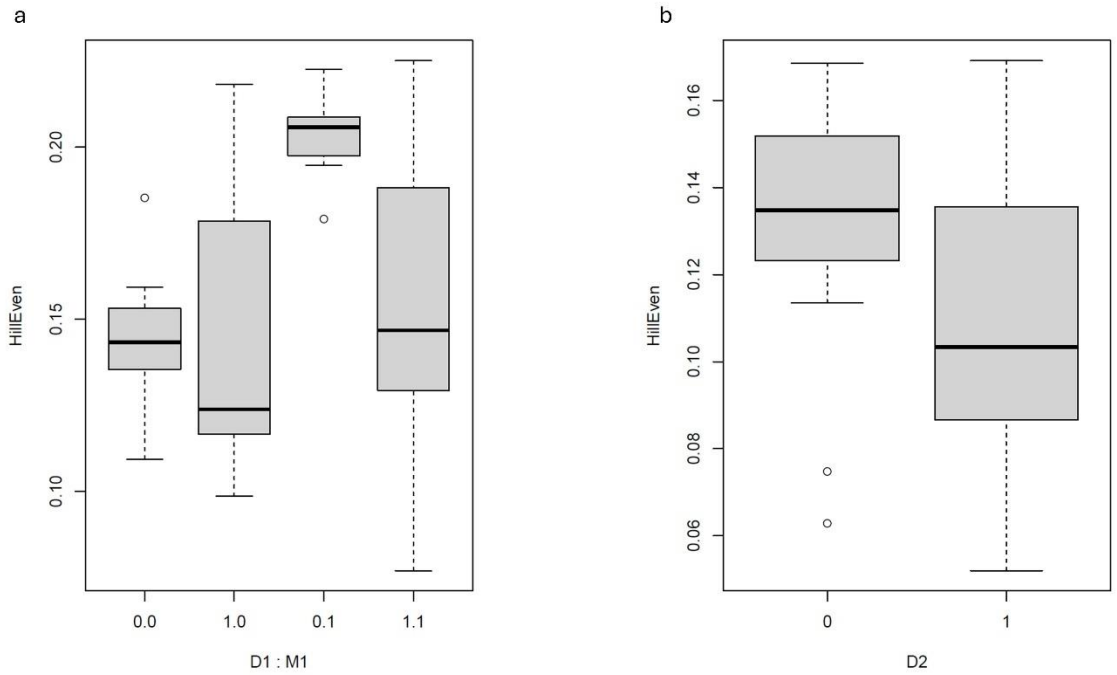

Figure S2: Boxplots showing the effects of interactions of M1, D1, D2, i.e. MeJA memory, drought memory and current drought, respectively in HillEven for (a) Positive mode and (b) negative mode in *F. rubra*. The X axis shows the levels of the interacting treatment, with 0 indicating absent and 1 present treatment (drought or MeJa).

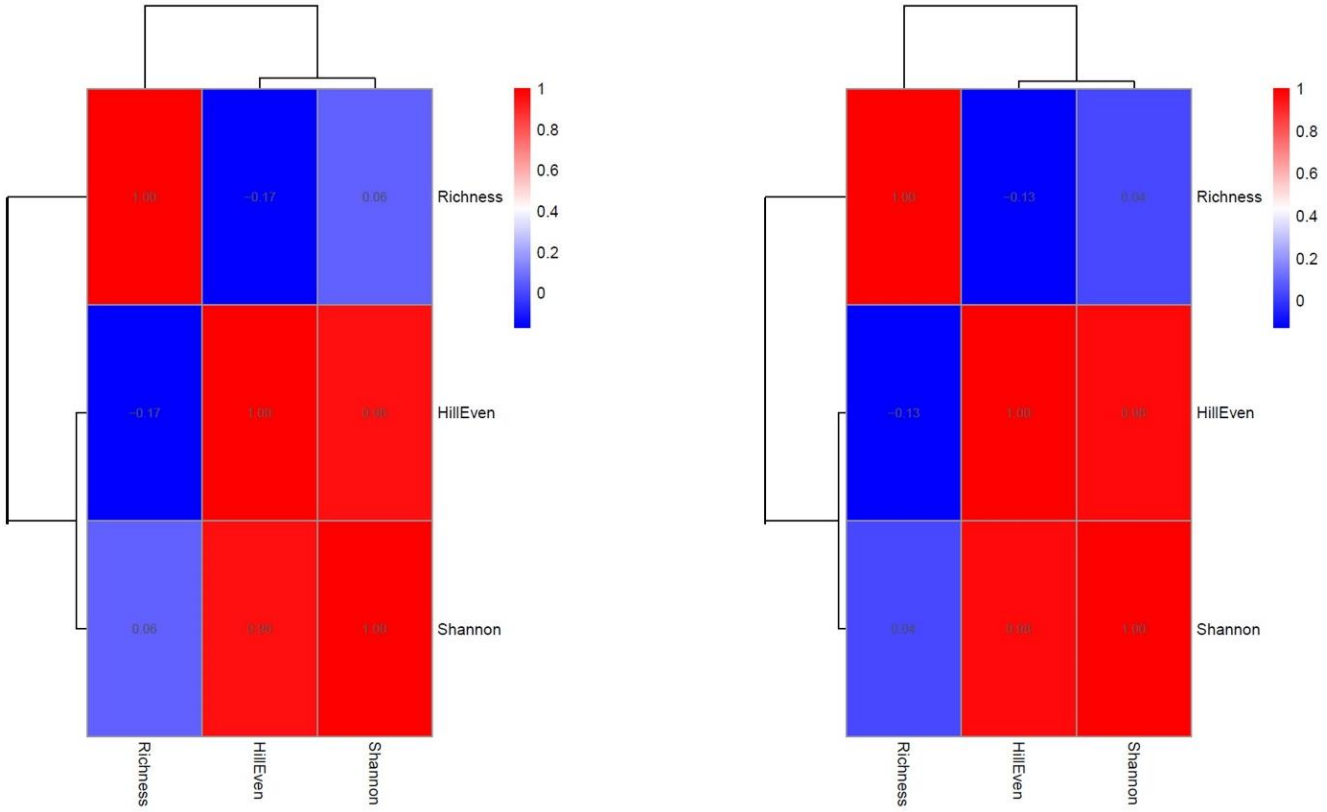

Figure S3: Correlation heatmap showing the relationship among Richness, Shannon diversity, and HillEvenness. Correlation coefficients are color-coded from dark blue (low correlation) to dark red (high correlation), with values displayed within each cell.

983

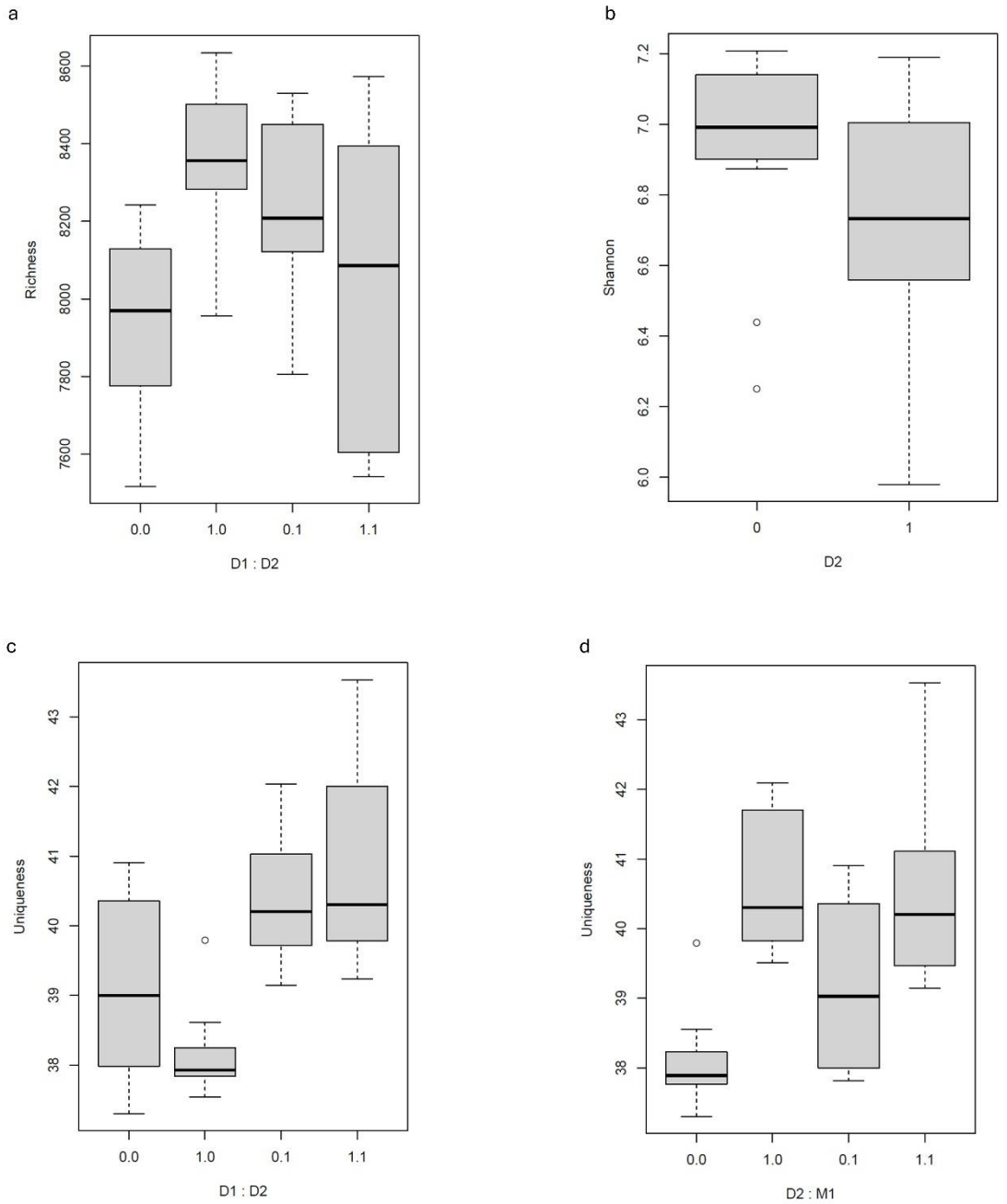

984

985 **Figure S4:** Boxplots showing the effects of interactions M1, D1, D2, i.e. MeJA memory,
986 drought memory and current drought, respectively, in positive mode for (a) Richness, (b)
987 Shannon diversity, and (c and d) Uniqueness in *F. rubra*. The X axis shows the levels of the
988 interacting treatment, with 0 indicating absent and 1 present treatment (drought or MeJA).

989

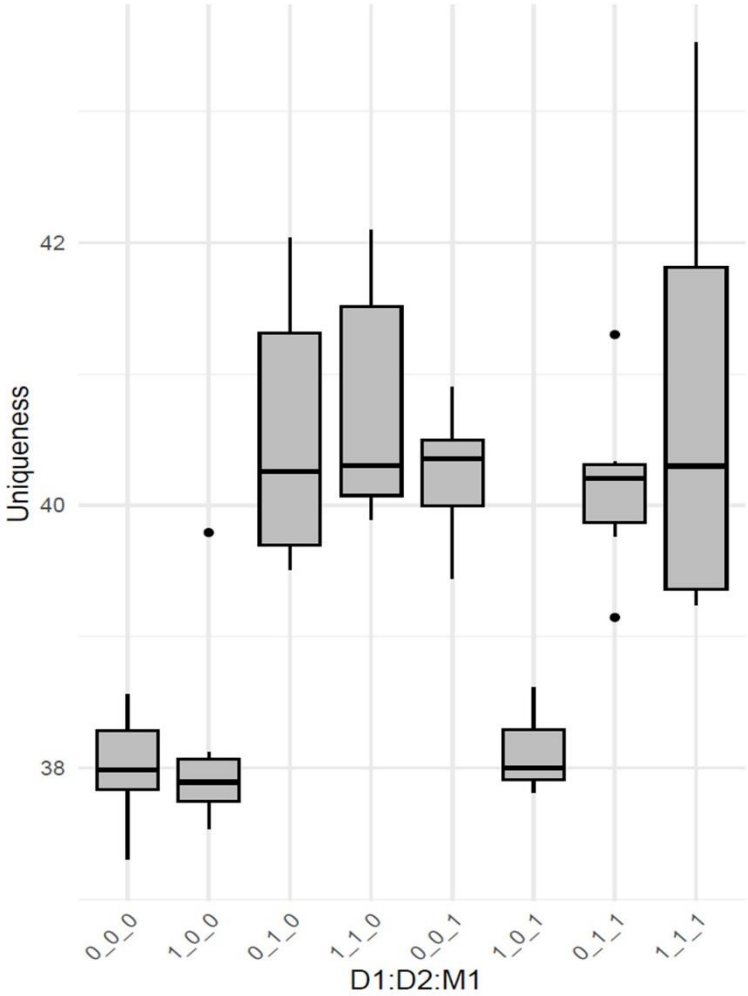

Figure S5: Boxplots show the distribution of metabolic uniqueness scores for each treatment group under negative ionization mode, representing the triple interaction of drought memory, current drought, and MeJA memory. In each code, a 1 in the first position indicates the presence of drought 1 (D1), a 1 in the second position indicates the presence of drought 2 (D2), and a 1 in the third position indicates the presence of the morphological modifier (M1). For example, 1_0_0 represents D1 only, 0_1_0 represents D2 only, and 1_1_1 represents a combination of D1, D2, and M1. The control group is 0_0_0, where no drought or modifier is applied.

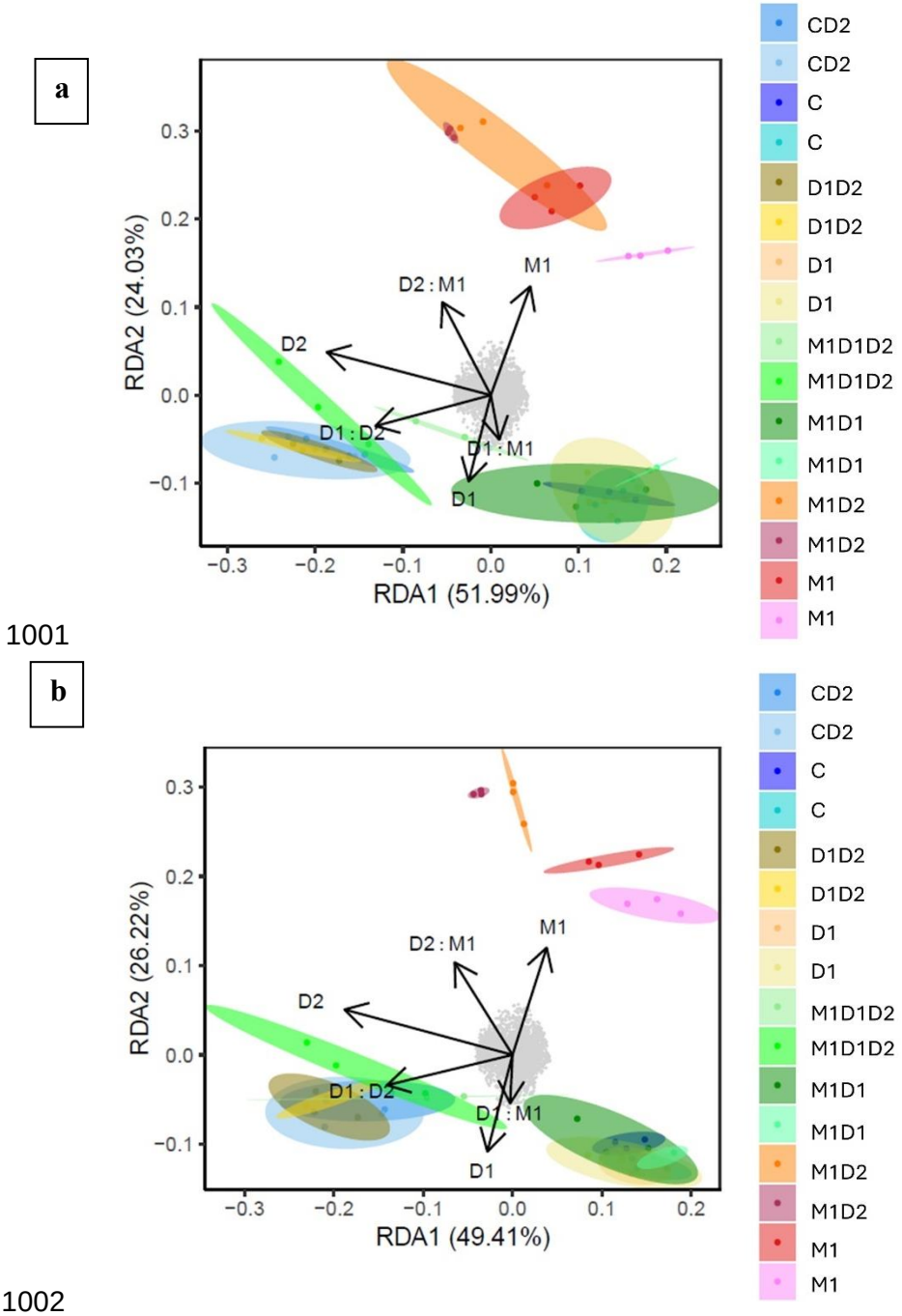

Figure S6: The RDA plots both ionization modes (**a**)positive and (**b**) negative, providing a clear view of the variation in metabolite profiles explained by M1, D1, D2, i.e., MeJA memory, drought memory and current drought, respectively.

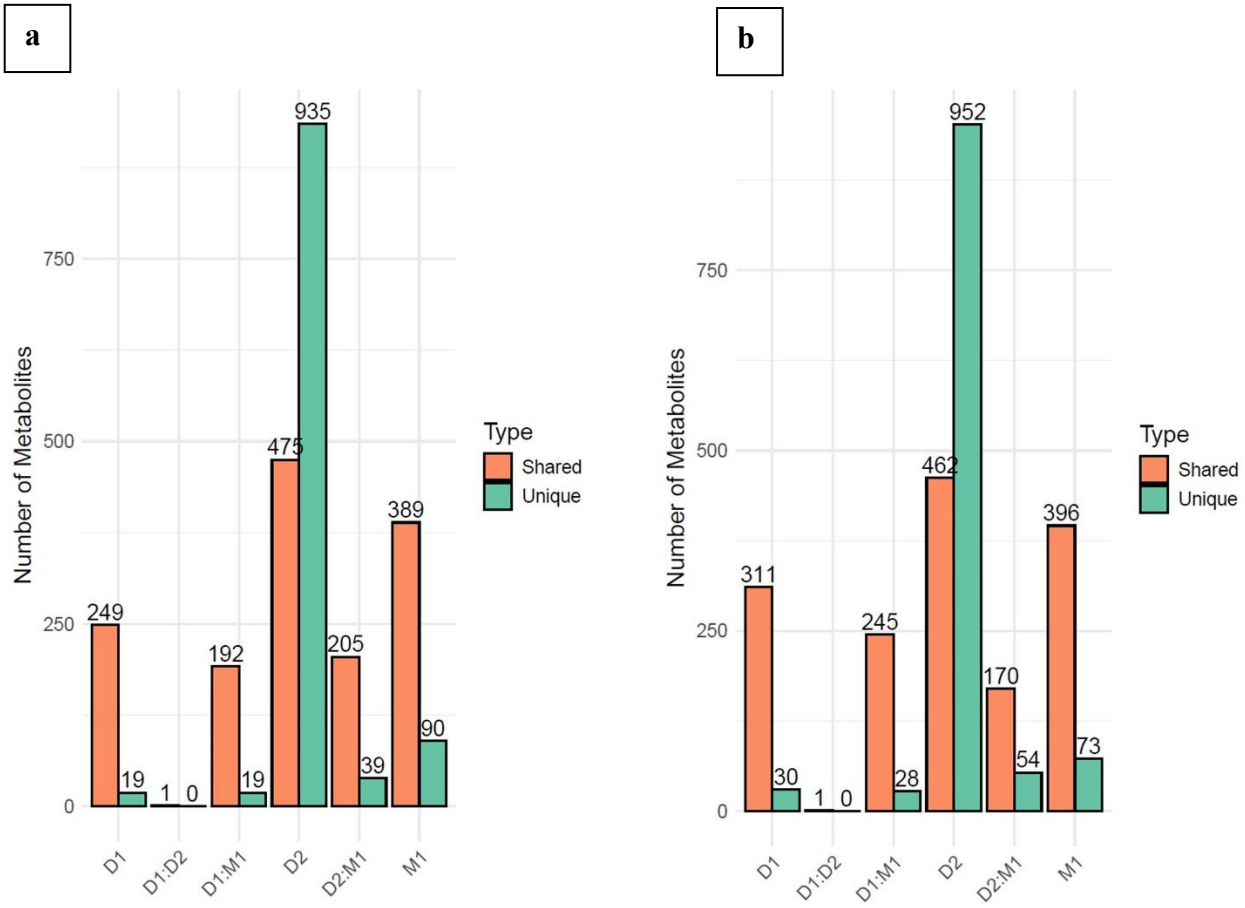

Figure S7: Bar plots representing the number of significant metabolites associated with drought memory (D1), MeJA memory (M1), current drought (D2), and their interactions (D1×D2, D1×M1, D2×M1) under positive ionization mode (a) and negative ionization mode (b). Each treatment or interaction is shown with two bars: shared metabolites (orange) indicate those common with other conditions, while unique metabolites (green) represent those specific to a given condition or interaction. The values above each bar indicate the exact number of metabolites in each category.

1017

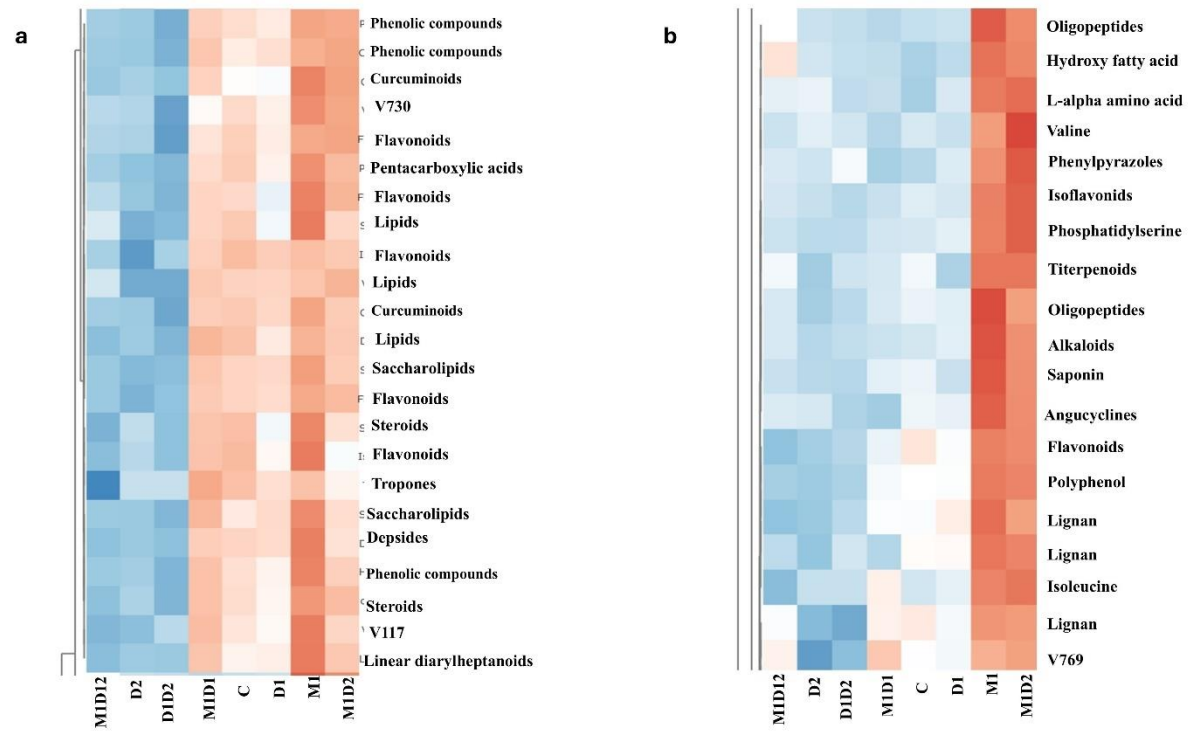
a
Phenolic compounds
Phenolic compounds
Curcuminoids
V730
Flavonoids
Pentacarboxylic acids
Flavonoids
Lipids
Flavonoids
Lipids
Curcuminoids
Lipids
Saccharolipids
Flavonoids
Steroids
Flavonoids
Tropones
Saccharolipids
Depsides
Phenolic compounds
Steroids
V117
Linear diarylheptanoids
M1D12
D2
D1D2
M1D1
C
D1
M1
M1D2
b
Oligopeptides
Hydroxy fatty acid
L-alpha amino acid
Valine
Phenylpyrazoles
Isoflavonids
Phosphatidylserine
Titerpenoids
Oligopeptides
Alkaloids
Saponin
Angucyclines
Flavonoids
Polyphenol
Lignan
Lignan
Isoleucine
Lignan
V769
M1D12
D2
D1D2
M1D1
C
D1
M1
M1D2

1018

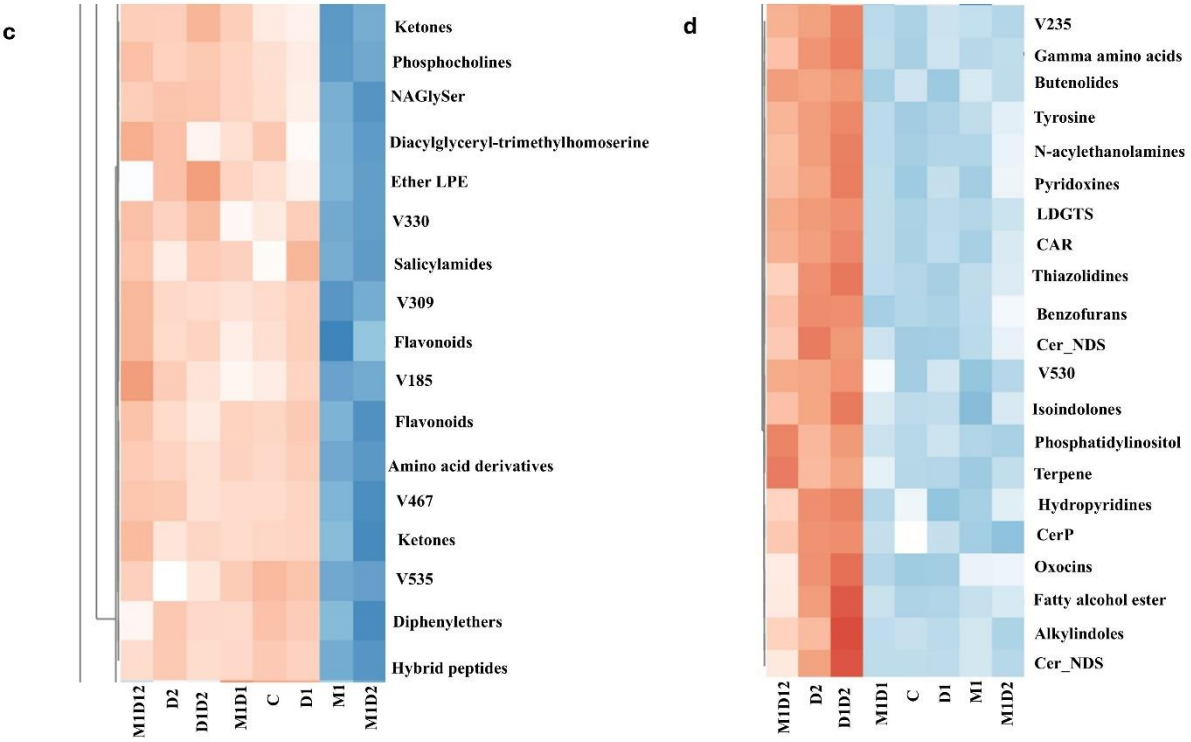
c
Ketones
Phosphocholines
NAGlySer
Diacylglyceryl-trimethylhomoserine
Ether LPE
V330
Salicylamides
V309
Flavonoids
V185
Flavonoids
Amino acid derivatives
V467
Ketones
V535
Diphenylethers
Hybrid peptides
M1D12
D2
D1D2
M1D1
C
D1
M1
M1D2
d
V235
Gamma amino acids
Butenolides
Tyrosine
N-acylethanolamines
Pyridoxines
LDGTS
CAR
Thiazolidines
Benzofurans
Cer_NDS
V530
Isoindolones
Phosphatidylinositol
Terpene
Hydropyridines
CerP
Oxocins
Fatty alcohol ester
Alkylindoles
Cer_NDS
M1D12
D2
D1D2
M1D1
C
D1
M1
M1D2

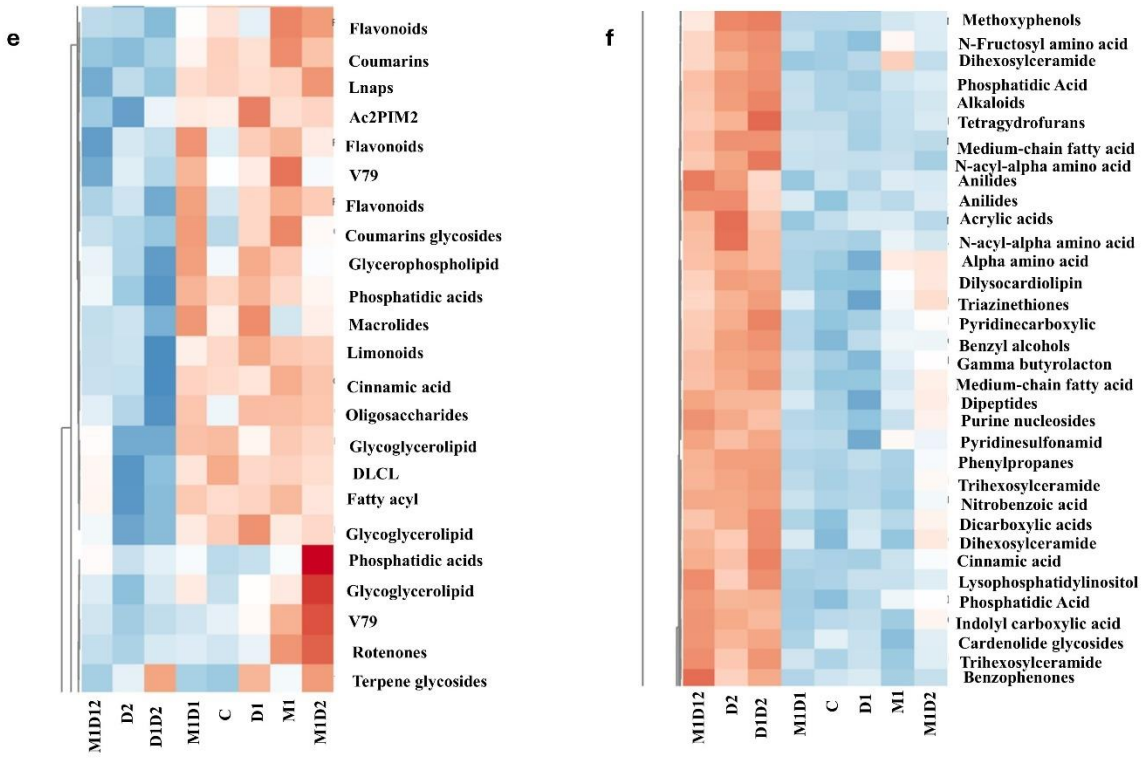

Figure S8: Heatmap displaying the scaled intensity values of differentially accumulated metabolites across various treatment groups in *F. rubra* (M1, D1, D2, i.e. MeJA memory, drought memory and current drought respectively), others are the plants which got combination M1, D2 and D2 treatment, while missing code in combination indicates that plants where not treated by the given treatment. C indicates Control, i.e., no drought or MeJa treatment memory, and in well-watered conditions. Heatmap a to d shows cluster 1 to 4, respectively for positive mode, while heatmap e and f shows cluster 1 and 2, respectively for negative mode